

Gravitational waves from bubble walls

Ariel Mégevand* and Federico Agustín Membiela†

IFIMAR (CONICET-UNMdP)

*Departamento de Física, Facultad de Ciencias Exactas y Naturales,
UNMdP, Deán Funes 3350, (7600) Mar del Plata, Argentina*

Abstract

We present a general method for computing the gravitational radiation arising from the motion of bubble walls or thin fluid shells in cosmological phase transitions. We discuss the application of this method to different wall kinematics. In particular, we derive general expressions for the bubble collision mechanism in the envelope approximation and the so-called bulk flow model, and we also consider deformations from the spherical bubble shape. We calculate the gravitational wave spectrum for a specific model of deformations on a definite size scale, which gives a peak away from that of the bubble collision mechanism.

1 Introduction

A phase transition of the Universe may give rise to gravitational waves (GWs) [1]. In particular, a first-order phase transition occurring at the electroweak scale gives naturally a GW spectrum which may be observable by the space-based interferometer LISA [2]. A first-order phase transition occurs via the nucleation and expansion of bubbles of a stable phase into a metastable one. In general, the phase transition is modeled with a scalar order-parameter field $\phi(\mathbf{x}, t)$ which couples to a relativistic fluid representing the plasma. A bubble corresponds to a configuration in which the scalar field takes the stable-phase value in some region, while outside this region it takes the value corresponding to the metastable phase (usually, $\phi = 0$). The interfaces or bubble walls propagate in the hot plasma. In many cases, they reach a terminal velocity due to the friction with the plasma (see, e.g., [3–9]). Alternatively, the walls may exhibit runaway behavior [10–12] and propagate with velocity $v = 1$ like in a vacuum phase transition. On the other hand, it has been shown that walls which propagate as subsonic deflagrations are unstable below

*Member of CONICET, Argentina. E-mail address: megevand@mdp.edu.ar

†Member of CONICET, Argentina. E-mail address: membiela@mdp.edu.ar

a certain critical velocity [13–16]. This instability causes the exponential growth of wall deformations as well as turbulent fluid motions near the walls.

Thus, the bubble walls may generate GWs in several ways. In the bubble collision mechanism [17, 18], the gravitational radiation is produced directly by the wall motion. Other mechanisms, such as turbulence [19–27] and sound waves [28–34], originate in the bulk fluid motions caused by the walls. Neither of these mechanisms take into account the possibility of wall deformations or the fluid motions caused by hydrodynamic instabilities.

The original calculation method for the bubble-collision mechanism is called the envelope approximation [35]. This approach consists in simulating the nucleation and expansion of spherical bubbles and considering only their walls as sources of GWs. The walls are assumed to be infinitely-thin and to disappear where bubbles overlap. The expansion of these spheres is followed until the end of the phase transition. The envelope approximation has also been used to compute the gravitational radiation from bulk fluid motions, assuming that the fluid is concentrated in thin shells next to the walls [19, 36]. In Ref. [37] it was pointed out that most of the calculations with the envelope approximation can be done analytically. The technique is based on a previous analytic approach [38], where the ensemble average of the source is taken. A similar approach was used more recently to consider thin fluid shells which persist after the walls collide [39]. This modification of the envelope approximation was called the bulk flow model in [40], where it was considered with the approach of simulating the formation and expansion of the thin fluid shells.

In the present paper we introduce a general method for calculating the GW spectrum from thin walls or fluid shells, which allows to consider different wall dynamics. Our approach is a hybrid between the one used in Refs. [35, 36] and that of Refs. [37, 38]. To illustrate the method, we derive expressions for the envelope approximation and the bulk flow model, which we compare with previous approaches. We also derive general expressions for arbitrary wall deformations and consider a particular example, in which we model deformations on a given length scale. This introduces a peak in the GW spectrum at a higher frequency than the usual generation mechanisms.

The plan is as follows. In the next section we introduce our general approach to the calculation of gravitational waves. In Sec. 3 we discuss the envelope approximation. In Sec. 4 we consider the bulk flow model. In Sec. 5 we address the case of wall deformations, and in Sec. 6 we discuss a specific model. We summarize our conclusions in Sec. 7. A detailed comparison of our approach with previous ones can be found in appendix A, while appendices B-D contain details on the calculations.

2 Bubble kinematics and gravitational waves

It is reasonable to assume that bubbles are initially spherical. However, since a spherical source does not radiate, a bubble must lose this symmetry in order to produce GWs. In the envelope approximation or in the bulk flow model, this happens as the bubbles collide and the bubble walls or fluid shells carry different surface energy density in their collided and uncollided parts. In contrast, a non-spherical bubble does not need to be collided to

generate GWs. Besides the already mentioned hydrodynamic instabilities, deformations can arise due to bubble collisions or other interactions. In particular, the inhomogeneous reheating due to shock fronts preceding deflagration fronts may cause velocity variations along a given bubble wall.

On the other hand, for the development of the phase transition it is simpler to model the bubbles as overlapping spheres, and we shall use this approximation (we shall take into account deformations only as a source of GWs). Assuming a homogeneous rate $\Gamma(t)$ per unit time per unit volume and a homogeneous wall velocity $v(t)$, a relatively simple statistical treatment of the phase transition is possible [41–43]. We shall ignore for simplicity the scale factor (which is valid if the transition is short enough), and we shall also make the usual approximation of neglecting the initial bubble size. Then, the radius of a bubble which nucleated at time t_N and expanded until time t is given by

$$R(t_N, t) = \int_{t_N}^t v(t'') dt''. \quad (1)$$

Taking into account bubble overlapping, the average fraction of volume remaining in the high-temperature phase at time t is given by $f_+(t) = e^{-I(t)}$, with

$$I(t) = \int_{-\infty}^t dt'' \Gamma(t'') \frac{4\pi}{3} R(t'', t)^3. \quad (2)$$

The lower limit of integration can be replaced with the time at which the critical temperature is reached, since the nucleation rate vanishes before that.

The relevant quantity in the computation of gravitational waves is the stress-energy tensor $T_{ij}(t, \mathbf{x})$ of the source. For the mechanism of bubble collisions in the envelope approximation, there have been essentially two different approaches. In numerical simulations such as those of Refs. [35, 36], the radiated energy is considered in the wave zone approximation. The stress-energy tensor is decomposed as a sum over bubbles, and the Fourier transform of each contribution is considered. A certain number of bubbles is nucleated, and then the result is summed and averaged over realizations of the phase transition. On the other hand, in the semi-analytic approach introduced in Refs. [37, 38], the evolution of the metric perturbations in Fourier space is calculated and linked to the source, and then the ensemble average is taken. This calculation involves the Fourier transform of the average $\langle T_{ij}(t, \mathbf{x}) T_{kl}(t', \mathbf{x}') \rangle$, and this quantity is related to the probability for the presence of bubble walls at the points (t, \mathbf{x}) , (t', \mathbf{x}') . The two approaches are of course equivalent. We compare them in some detail in appendix A. Here we shall use a hybrid approach. We shall decompose the stress-energy tensor into individual bubbles like in Ref. [35], but we shall consider analytically the ensemble average. This method will allow us to obtain general results in fewer steps, and is also suitable for considering more general wall dynamics than that of bubble expansion.

We begin by writing the gravitational wave power spectrum for a large volume V in the form

$$\frac{d\rho_{GW}}{d\ln\omega} = \frac{4G\omega^3}{\pi} \int_{-\infty}^{\infty} dt \int_t^{\infty} dt' \cos[\omega(t-t')] \Pi(t, t', \omega), \quad (3)$$

where

$$\Pi(t, t', \omega) \equiv \frac{1}{V} \Lambda_{ij,kl}(\hat{n}) \left\langle \tilde{T}_{ij}(t, \omega \hat{n}) \tilde{T}_{kl}(t', \omega \hat{n})^* \right\rangle. \quad (4)$$

Here, the symbol $\langle \rangle$ denotes ensemble average, $\Lambda_{ij,kl}(\hat{n})$ is the transverse-traceless projection tensor

$$\Lambda_{ij,kl} = \delta_{ik}\delta_{jl} - \frac{1}{2}\delta_{ij}\delta_{kl} - \hat{n}_j\hat{n}_l\delta_{ik} - \hat{n}_i\hat{n}_k\delta_{jl} + \frac{1}{2}\hat{n}_k\hat{n}_l\delta_{ij} + \frac{1}{2}\hat{n}_i\hat{n}_j\delta_{kl} + \frac{1}{2}\hat{n}_i\hat{n}_j\hat{n}_k\hat{n}_l, \quad (5)$$

\hat{n} is the direction of observation, and \tilde{T}_{ij} are the spatial components of the Fourier transform of the stress-energy tensor,

$$\tilde{T}_{ij}(t, \omega \hat{n}) = \int_V d^3x e^{-i\omega \hat{n} \cdot \mathbf{x}} T_{ij}(t, \mathbf{x}). \quad (6)$$

In appendix A we derive these formulas and compare with the aforementioned approaches. We also show that homogeneity and isotropy imply that the quantity $\Pi(t, t', \omega)$ is real, does not depend on \hat{n} , and satisfies $\Pi(t, t', \omega) = \Pi(t', t, \omega)$.

From now on we shall denote the total energy-momentum tensor of the system as T_{ij}^{tot} , while T_{ij} will denote the contribution from a single bubble. Each bubble gives rise to different GW sources (the wall motion, bulk fluid motions, etc.). We shall consider cases in which the GW sources which originate in different bubbles do not overlap, so that the total energy-momentum tensor is of the form

$$T_{ij}^{\text{tot}}(t, \mathbf{x}) = \sum_n T_{ij}^{(n)}(r_n, \hat{r}_n, t), \quad (7)$$

where $r_n = |\mathbf{x} - \mathbf{x}_n|$, $\hat{r}_n = (\mathbf{x} - \mathbf{x}_n)/r_n$, and \mathbf{x}_n is the position of the center of the n th bubble. In this description, we define the bubble as a sphere centered at \mathbf{x}_n and with a radius $R(t_N^{(n)}, t)$ given by Eq. (1), where $t_N^{(n)}$ is the nucleation time. However, the support of the associated contribution $T_{ij}^{(n)}$ might be larger or smaller than this sphere, depending on the source we consider.

Inserting Eq. (7) in Eq. (6), we obtain

$$\tilde{T}_{ij}^{\text{tot}}(t, \omega \hat{n}) = \sum_n e^{-i\omega \hat{n} \cdot \mathbf{x}_n} \tilde{T}_{ij}^{(n)}(t, \omega \hat{n}), \quad (8)$$

with

$$\tilde{T}_{ij}^{(n)}(t, \omega \hat{n}) = \int r^2 dr \int d\hat{r} e^{-i\omega \hat{n} \cdot \mathbf{r}} T_{ij}^{(n)}(r, \hat{r}, t), \quad (9)$$

where the origin of the radial variable r is the center of the n th bubble, and we use the notation $d\hat{r} \equiv \sin\theta d\theta d\phi$. We have to compute the quantity (4),

$$\Pi(t, t', \omega) = \frac{1}{V} \left\langle \sum_n \sum_m e^{-i\omega \hat{n} \cdot (\mathbf{x}_n - \mathbf{x}_m)} \Lambda_{ij,kl}(\hat{n}) \tilde{T}_{ij}^{(n)}(t, \omega \hat{n}) \tilde{T}_{kl}^{(m)}(t', \omega \hat{n})^* \right\rangle. \quad (10)$$

It is convenient to calculate separately the contributions of $m = n$ and those of $m \neq n$, since the correlations within a given bubble are different from those between different bubbles. Moreover, both contributions scale with the volume V [44], in spite of the fact that the number of terms in the double sum scales with V^2 . This naturally decomposes Eq. (10) into single-bubble and two-bubble contributions, and we shall use indices s, d for them, like in the treatment of Ref. [37].

Let us first consider the single-bubble contribution,

$$\Pi^{(s)}(t, t', \omega) = \Lambda_{ij,kl}(\hat{n}) \frac{1}{V} \left\langle \sum_n \tilde{T}_{ij}^{(n)}(t, \omega \hat{n}) \tilde{T}_{kl}^{(n)}(t', \omega \hat{n})^* \right\rangle. \quad (11)$$

For each term, t and t' are two instants in the history of the same bubble (labeled by n), which was nucleated at some time $t_N^{(n)}$ previous to both t and t' . We can think of the ensemble as a large number of realizations of the phase transition. For each realization, we may arrange the terms of the sum in (11) into groups of bubbles nucleated in the same neighborhood around the same time. Thus, the average in Eq. (11) separates into a sum of averages, each of which involves only bubbles nucleated in a certain region and time. The group of bubbles nucleated around a given position \mathbf{x}_N and in a time interval $[t_N, t_N + dt_N]$ will have, on average, a number of members dN_b given by

$$dN_b = \Gamma(t_N) f_+(t_N) d^3 x_N dt_N. \quad (12)$$

If we pick one bubble of this group from each realization of the phase transition, we may use such a collection to formally define the average of the quantity $\tilde{T}_{ij} \tilde{T}_{kl}^*$ for a single bubble. By homogeneity, the resulting average does not depend on the bubble position \mathbf{x}_N , and we denote it as¹

$$\left\langle \tilde{T}_{ij}(t, \omega \hat{n}) \tilde{T}_{kl}(t', \omega \hat{n})^* \right\rangle^{(s)}(t_N). \quad (13)$$

Multiplying by the average number dN_b and integrating over the nucleation position, the volume factor in Eq. (11) cancels and we obtain

$$\Pi^{(s)}(t, t', \omega) = \int_{-\infty}^t dt_N \Gamma(t_N) f_+(t_N) \Lambda_{ij,kl}(\hat{n}) \left\langle \tilde{T}_{ij}(t, \omega \hat{n}) \tilde{T}_{kl}(t', \omega \hat{n})^* \right\rangle^{(s)}. \quad (14)$$

The nucleation time must be integrated from $-\infty$ (or from t_c) to the smallest of t and t' , which, according to Eq. (3)², is t .

Now let us consider the two-bubble contribution, which is given by Eq. (10) with $n \neq m$. We may divide each sum into groups of bubbles nucleated in small neighborhoods around positions \mathbf{x}_N and \mathbf{x}'_N and in small time intervals around t_N and t'_N . However, by homogeneity, the contribution of a pair of neighborhoods to the average will depend

¹Notice that \tilde{T}_{ij} is given by Eq. (9), where the bubble index must be dropped when taking the average.

²If we use instead the symmetric expression (149) of appendix A for $d\rho_{GW}/d\ln\omega$, the limit of integration in (14) must be replaced by $t_m = \min\{t, t'\}$.

only on the relative position $\mathbf{l} = \mathbf{x}'_N - \mathbf{x}_N$. If we pick, from each realization of the phase transition, one such pair of bubbles and average the quantity $\tilde{T}_{ij}\tilde{T}_{kl}^*$, we obtain the two-bubble ensemble average

$$\left\langle \tilde{T}_{ij}(t, \omega \hat{n}) \tilde{T}_{kl}(t', \omega \hat{n})^* \right\rangle^{(d)}(t_N, t'_N, \mathbf{l}). \quad (15)$$

To calculate the double sum of Eq. (10), we must integrate over \mathbf{x}_N and \mathbf{x}'_N , which gives a factor of V and an integral over \mathbf{l} . The volume factor cancels, and we obtain

$$\begin{aligned} \Pi^{(d)}(t, t', \omega) &= \int_{-\infty}^t dt_N \Gamma(t_N) f_+(t_N) \int_{t_c}^{t'} dt'_N \Gamma(t'_N) f_+(t'_N) \\ &\quad \times \int d^3l e^{i\omega \hat{n} \cdot \mathbf{l}} \Lambda_{ij,kl}(\hat{n}) \left\langle \tilde{T}_{ij}(t, \omega \hat{n}) \tilde{T}_{kl}(t', \omega \hat{n})^* \right\rangle^{(d)}. \end{aligned} \quad (16)$$

Notice that, in this expression, the contribution of correlations between bubbles of the same age is negligible, since it is of order $(dN_b)^2$. Nevertheless, single-bubble correlations give the finite contribution (14).

The expressions (14) and (16) will be valid whenever the quantities T_{ij} belonging to different bubbles have little overlapping. For instance, in the case of hydrodynamic instabilities which may be developed by deflagration walls, unstable modes grow exponentially in the surrounding fluid (besides a corrugation of the wall). These perturbations break the spherical symmetry, so GWs may be produced well before bubbles begin to overlap. On the other hand, if the energy-momentum tensor is concentrated in thin shells, the overlapping will be negligible even when the bubbles overlap significantly.

3 The envelope approximation

A bubble is a configuration in which the scalar field ϕ has a non-vanishing constant value inside a certain domain and falls to zero outside this region. The non-diagonal components of T_{ij} for the scalar field are given by $T_{ij}^\phi = \partial_i \phi \partial_j \phi$, and are non-vanishing only where ϕ has a spatial variation, which is, by definition, the bubble wall. For a spherical configuration of the form $\phi = \phi(r)$, we have $T_{ij}^\phi = \hat{r}_i \hat{r}_j (\partial_r \phi)^2$. More specifically, we shall write the field profile of the bubble in the form

$$\phi(\mathbf{x}, t) = \phi_0(r - R), \quad (17)$$

where ϕ_0 is the solution of the 1-dimensional problem (a tanh profile is often used as an approximation), and $R \equiv R(t_N, t)$ is the position of the wall, which is given by Eq. (1). We shall use the approximation of infinitely thin walls, which we implement by writing $\phi'_0(x)^2 = \sigma_0 \delta(x)$, where $\phi'_0 \equiv d\phi_0/dx$, and $\sigma_0 = \int \phi_0'^2 dx$ is the surface tension. This quantity can be computed from the field profile, and we shall regard it as a free parameter. In the envelope approximation, we assume that the wall just disappears in the intersections with other bubbles. Thus, we have

$$T_{ij}^\phi = \hat{r}_i \hat{r}_j \sigma_0 \delta(r - R) 1_S(\hat{r}), \quad (18)$$

where 1_S is the indicator function for the uncollided bubble surface S at time t ,

$$1_S(\hat{r}) = \begin{cases} 1 & \text{if } R\hat{r} \text{ is uncollided,} \\ 0 & \text{otherwise.} \end{cases} \quad (19)$$

Therefore, the quantity \tilde{T}_{ij} defined by Eq. (9) becomes

$$\tilde{T}_{ij}(t, \omega \hat{n}) = \sigma_0 R^2 \int d\hat{r} e^{-i\omega R \hat{n} \cdot \hat{r}} \hat{r}_i \hat{r}_j 1_S(\hat{r}). \quad (20)$$

We shall now replace the constant σ_0 by a variable surface energy density σ in order to take into account the fact that energy may accumulate in the wall. To obtain this replacement formally, we may replace Eq. (17) by $\phi(\mathbf{x}, t) = \phi_0(\gamma(r - R))$, where $\gamma = 1/\sqrt{1 - v^2}$, so that the contraction of the wall width is taken into account (see, e.g., [45, 46]). This gives $(\partial_r \phi)^2 = \gamma^2 \sigma_0 \delta(\gamma(r - R))$, which results in a single factor γ in Eq. (20), corresponding to a surface energy density $\sigma = \gamma \sigma_0$. This factor grows with time if the wall is accelerated³. In a vacuum transition, all of the released energy goes to the wall, so the surface energy $4\pi R^2 \sigma$ is given by the released energy $(4\pi/3)R^3 \rho_{\text{vac}}$. This gives $\sigma = (\rho_{\text{vac}}/3)R$.

In contrast, if the phase transition occurs in a hot plasma, the wall may reach a constant velocity. In this case, most of the released energy goes to the fluid, and we have $\sigma = \sigma_0$, which will give a much lower GW signal⁴. Nevertheless, a fluid profile forms next to the bubble wall, and the envelope approximation has been used for this case, assuming that the energy is concentrated in a thin shell. For the fluid, the relevant part of the energy-momentum tensor is $T_{ij}^{\text{fl}} = w \gamma_{\text{fl}}^2 v_{\text{fl}i} v_{\text{fl}j}$, where w is the enthalpy density, v_{fl} is the fluid velocity, and $\gamma_{\text{fl}} = 1/\sqrt{1 - v_{\text{fl}}^2}$. For a spherical configuration, the velocity is of the form $\mathbf{v}_{\text{fl}} = v_{\text{fl}}(r)\hat{r}$ and the enthalpy density is of the form $w = w(r)$. Therefore, we have $T_{ij}^{\text{fl}} = \hat{r}_i \hat{r}_j w \gamma_{\text{fl}}^2 v_{\text{fl}}^2$, which is of the same form of T_{ij}^{ϕ} , namely, $f(r)\hat{r}_i \hat{r}_j$, although the function $f(r)$ has a wider support for the fluid. Assuming anyway a thin fluid shell, the approximation (20) can be used, with σ_0 replaced by

$$\sigma = (\kappa \rho_{\text{vac}}/3)R, \quad (21)$$

where κ is an efficiency factor accounting for the fraction of energy which goes to bulk fluid motions [19]. It can be calculated from the fluid velocity profile (see, e.g., [46–54]), and we shall consider it as a free parameter here. In an intermediate case in which the wall is accelerated but a part of the energy goes to the fluid, there are different efficiency

³It can be seen [35] that, in the relativistic limit, the kinetic and gradient energy terms inside the wall, $\frac{1}{2}(\partial_r \phi)^2$, $\frac{1}{2}(\partial_t \phi)^2$, become equal in a short time, and both terms grow with t^3 while the potential energy becomes negligible. Therefore $\sigma = \int (\partial_r \phi)^2 dr = \gamma \sigma_0$ gives indeed the energy density which is accumulated inside the wall.

⁴Dimensionally, we have $\sigma_0 \sim T^3$, $\rho_{\text{vac}} \sim T^4$, and $R \sim M_P/T^2$, where M_P is the Planck mass. Hence there is an enhancement of order M_P/T for $\sigma = (\rho_{\text{vac}}/3)R$ with respect to $\sigma = \sigma_0$.

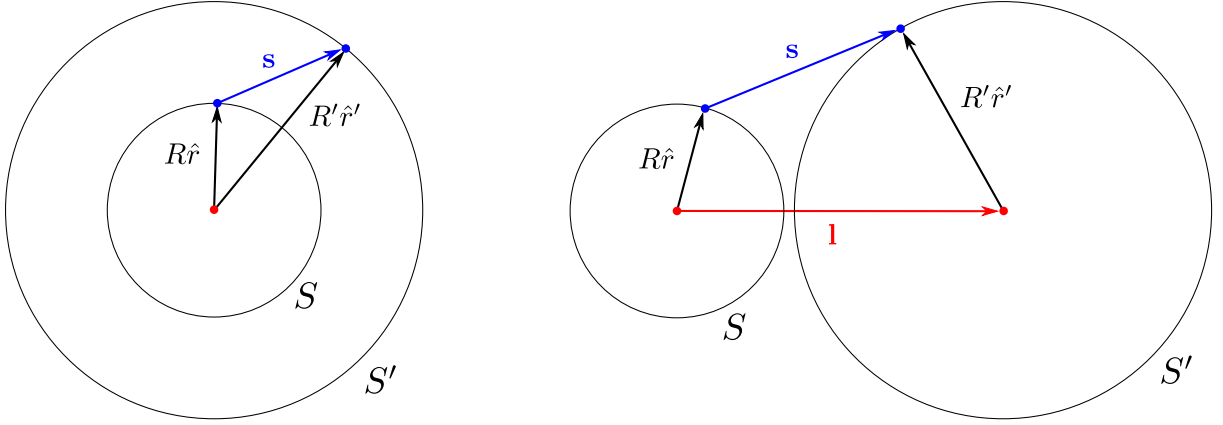


Figure 1: Relations between the vectors $R\hat{r}$, $R'\hat{r}'$, \mathbf{s} , and \mathbf{l} . Left: single-bubble case. Right: two-bubble case.

factors for the wall and for the fluid [55,56]. In the envelope approximation, κ represents the sum of these contributions⁵.

Inserting Eq. (20) in Eqs. (14) and (16), we obtain

$$\Pi^{(s)} = \int_{-\infty}^t dt_N \Gamma(t_N) f_+(t_N) \sigma R^2 \sigma' R'^2 \int d\hat{r} \int d\hat{r}' e^{i\omega\hat{n}\cdot\mathbf{s}} \Lambda_{ij,kl} \hat{r}_i \hat{r}_j \hat{r}'_k \hat{r}'_l \langle 1_S(\hat{r}) 1_{S'}(\hat{r}') \rangle \quad (22)$$

and

$$\begin{aligned} \Pi^{(d)} = & \int_{-\infty}^t dt_N \Gamma(t_N) f_+(t_N) \sigma R^2 \int_{-\infty}^{t'} dt'_N \Gamma(t'_N) f_+(t'_N) \sigma' R'^2 \\ & \times \int d^3l \int d\hat{r} \int d\hat{r}' e^{i\omega\hat{n}\cdot\mathbf{s}} \Lambda_{ij,kl} \hat{r}_i \hat{r}_j \hat{r}'_k \hat{r}'_l \langle 1_S(\hat{r}) 1_{S'}(\hat{r}') \rangle. \quad (23) \end{aligned}$$

Here, R' means $R(t_N, t')$ for the single-bubble contribution and $R(t'_N, t')$ for the two-bubble contribution, while S' is the uncollided surface of the corresponding bubble at time t' . The vector $\mathbf{s} = \mathbf{l} + R'\hat{r}' - R\hat{r}$ (with $\mathbf{l} = \mathbf{0}$ in the single-bubble case) connects the points p and p' on the surfaces S and S' which are determined by the directions \hat{r} and \hat{r}' , respectively (see Fig. 1). The quantity $\Lambda_{ij,kl} \hat{r}_i \hat{r}_j \hat{r}'_k \hat{r}'_l$ can be written as

$$\begin{aligned} \Lambda(\hat{n})_{ij,kl} \hat{r}_i \hat{r}_j \hat{r}'_k \hat{r}'_l = & (\hat{r} \cdot \hat{r}')^2 - \frac{1}{2} - 2(\hat{r} \cdot \hat{r}')(\hat{n} \cdot \hat{r})(\hat{n} \cdot \hat{r}') \\ & + \frac{1}{2}(\hat{n} \cdot \hat{r}')^2 + \frac{1}{2}(\hat{n} \cdot \hat{r})^2 + \frac{1}{2}(\hat{n} \cdot \hat{r})^2(\hat{n} \cdot \hat{r}')^2. \quad (24) \end{aligned}$$

⁵It is worth noticing that the usual assumption that κ and ρ_{vac} are constant parameters is an approximation (which we adopt here). The released energy ρ_{vac} depends on the temperature (which varies during the phase transition), while the efficiency factor κ depends also on the wall velocity. To take into account a varying transfer of energy to the wall, the released energy $\kappa \rho_{\text{vac}} \frac{4\pi}{3} R^3$ should be replaced by $\int_{t_N}^t 4\pi R^2 \kappa \rho_{\text{vac}} v dt''$.

On the other hand, the product $1_S(\hat{r})1_{S'}(\hat{r}')$ takes the value 1 if the points p and p' on each spherical surface are both uncollided and vanishes otherwise, so we have

$$\langle 1_S(\hat{r})1_{S'}(\hat{r}') \rangle = P_{uu}(\hat{r}, \hat{r}'), \quad (25)$$

where P_{uu} is the probability that both points are uncollided (at the corresponding times t and t').

The probability P_{uu} was considered in Ref. [44] (see [37] for related calculations). The result is different if the two points belong to the same bubble surface or to two different bubbles. In the single-bubble case, we have

$$P_{uu}^{(s)} = \exp[-I(t) - I(t') + I_{\cap}(t, t', s) + I(t_N)], \quad (26)$$

where the function $I(t)$ is defined in Eq. (2), and the quantity I_{\cap} is given (for $t < t'$) by

$$I_{\cap}(t, t', s) = \int_{-\infty}^t dt'' \Gamma(t'') V_{\cap}(t'', t, t', s). \quad (27)$$

Here, V_{\cap} is the volume of the intersection of two spheres centered at the points p and p' , of radii $r = R(t'', t)$ and $r' = R(t'', t')$, respectively. Their centers are separated by a distance $s = |\mathbf{s}|$, and the intersection volume is given by

$$V_{\cap} = \frac{\pi}{12}(r + r' - s)^2 \left[s + 2(r + r') - \frac{3(r - r')^2}{s} \right] \Theta(r + r' - s), \quad (28)$$

where Θ is the Heaviside step function⁶. In brief, the interpretation of Eq. (26) is the following (see [44] for details). The quantity $I(t)$ is related to the probability that the point p on S has been reached at time t by bubbles nucleated at times $t'' < t$. Such bubbles would have nucleated within the volume $V = \frac{4\pi}{3}R(t'', t)^3$ around p . Similarly, $I(t')$ corresponds to the probability for p' on S' , and depends on the volume $V' = \frac{4\pi}{3}R(t'', t')^3$. In order to avoid doubly counting bubbles which would affect both points, the intersection volume V_{\cap} must be subtracted. Finally, the bubble containing p and p' would not exist if a previous bubble were nucleated within a volume $V_N = \frac{4\pi}{3}R(t'', t_N)^3$ around its center. The term $I(t_N)$ takes into account that this volume must also be subtracted from the calculation. In the two-bubble case, the joint probability for the points p and p' to be uncollided is very similar,

$$P_{uu}^{(d)} = \exp[-I(t) - I(t') + I_{\cap}(t, t', s) + I(t_N) + I(t'_N)] \\ \times \Theta(|\mathbf{1} - R\hat{r}| - R(t'_N, t)) \Theta(|\mathbf{1} + R'\hat{r}'| - R(t_N, t')). \quad (29)$$

The main difference is that P_{uu} vanishes if the bubbles are so close that one of the points has been eaten by the other bubble. Thus, the Heaviside functions take care that the

⁶For $s \leq r' - r$ the intersection volume is actually given by $V_{\cap} = 4\pi r^3/3$. However, the point separation s is always greater than the difference $r' - r$. This holds also for the two-bubble case considered below, under the conditions imposed by the Heaviside functions in Eq. (29) [44].

distance from one of the points to the center of the other bubble be greater than the radius of the latter at the corresponding time.

Notice that the factors $e^{I(t_N)}$ and $e^{I(t'_N)}$ in Eqs. (26) and (29) will cancel with the factors $f_+(t_N)$ and $f_+(t'_N)$ in Eqs. (22) and (23). Thus, using also the surface energy density (21), we obtain

$$\begin{aligned} \Pi^{(s)}(t, t', \omega) &= \frac{\kappa^2 \rho_{\text{vac}}^2}{9} \int_{-\infty}^t dt_N \Gamma(t_N) R(t_N, t)^3 R(t_N, t')^3 \\ &\quad \times \int d\hat{r} \int d\hat{r}' e^{-I_{\text{tot}}(t, t', s)} e^{i\omega \hat{n} \cdot \mathbf{s}} (\Lambda_{ij,kl} \hat{r}_i \hat{r}_j \hat{r}'_k \hat{r}'_l), \end{aligned} \quad (30)$$

$$\begin{aligned} \Pi^{(d)}(t, t', \omega) &= \frac{\kappa^2 \rho_{\text{vac}}^2}{9} \int_{-\infty}^t dt_N \Gamma(t_N) R(t_N, t)^3 \int_{-\infty}^{t'} dt'_N \Gamma(t'_N) R(t'_N, t')^3 \\ &\quad \times \int d^3l \int d\hat{r} \int d\hat{r}' e^{-I_{\text{tot}}(t, t', s)} e^{i\omega \hat{n} \cdot \mathbf{s}} (\Lambda_{ij,kl} \hat{r}_i \hat{r}_j \hat{r}'_k \hat{r}'_l), \end{aligned} \quad (31)$$

where $I_{\text{tot}} \equiv I(t) + I(t') - I_{\cap}(t, t', s)$. The conditions imposed by the Heaviside functions (29) must be taken into account as limits of integration in Eq. (31). To simplify the angular integrations, we shall first average out the direction of observation \hat{n} (we can do that since the GW spectrum will not depend on \hat{n}). Thus, we make the replacement

$$e^{i\omega \hat{n} \cdot \mathbf{s}} \Lambda_{ij,kl}(\hat{n}) \hat{r}_i \hat{r}_j \hat{r}'_k \hat{r}'_l \rightarrow \frac{1}{4\pi} \int d\hat{n} e^{i\omega \hat{n} \cdot \mathbf{s}} \Lambda_{ij,kl}(\hat{n}) \hat{r}_i \hat{r}_j \hat{r}'_k \hat{r}'_l = \sum_{i=0}^2 C_i \frac{j_i(\omega s)}{(\omega s)^i}. \quad (32)$$

(the calculation is done in appendix B). Here, j_i are the spherical Bessel functions

$$j_0(x) = \frac{\sin x}{x}, \quad j_1(x) = \frac{\sin x - x \cos x}{x^2}, \quad j_2(x) = \frac{(3 - x^2) \sin x - 3x \cos x}{x^3}, \quad (33)$$

and the coefficients C_i are given by

$$C_0 = -\frac{1}{2} + \frac{(\hat{r} \cdot \hat{s})^2}{2} + \frac{(\hat{r}' \cdot \hat{s})^2}{2} + \frac{(\hat{r} \cdot \hat{s})^2 (\hat{r}' \cdot \hat{s})^2}{2} - 2(\hat{r} \cdot \hat{s})(\hat{r}' \cdot \hat{s})(\hat{r} \cdot \hat{r}') + (\hat{r} \cdot \hat{r}')^2, \quad (34)$$

$$C_1 = 1 - (\hat{r} \cdot \hat{s})^2 - (\hat{r}' \cdot \hat{s})^2 - 5(\hat{r} \cdot \hat{s})^2 (\hat{r}' \cdot \hat{s})^2 + 8(\hat{r} \cdot \hat{s})(\hat{r}' \cdot \hat{s})(\hat{r} \cdot \hat{r}') - 2(\hat{r} \cdot \hat{r}')^2, \quad (35)$$

$$C_2 = \frac{1 - 5(\hat{r} \cdot \hat{s})^2 - 5(\hat{r}' \cdot \hat{s})^2 + 35(\hat{r} \cdot \hat{s})^2 (\hat{r}' \cdot \hat{s})^2}{2} - 10(\hat{r} \cdot \hat{s})(\hat{r}' \cdot \hat{s})(\hat{r} \cdot \hat{r}') + (\hat{r} \cdot \hat{r}')^2. \quad (36)$$

For the single-bubble contribution (30) we have $\mathbf{s} = R'\hat{r}' - R\hat{r}$, so all the terms in (34)-(36) can be written in terms of a single cosine, namely, $c \equiv \hat{r} \cdot \hat{r}'$, which, furthermore, is related to s through

$$s^2 = R^2 + R'^2 - 2RR'c. \quad (37)$$

We thus obtain (see appendix B)

$$\frac{1}{4\pi} \int d\hat{n} e^{i\omega \hat{n} \cdot \mathbf{s}} (\Lambda_{ij,kl} \hat{r}_i \hat{r}_j \hat{r}'_k \hat{r}'_l) = \sum_{i=0}^2 \frac{P_i(s, R, R') j_i(\omega s)}{32R^2 R'^2 s^4 (\omega s)^i}, \quad (38)$$

where the P_i are homogeneous polynomials of degree 8, which have simpler expressions in terms of $R_+ = R' + R$ and $R_- = R' - R = R(t, t')$,

$$P_0(R_+, R_-, s) = (s^2 - R_-^2)(s^2 - R_+^2)^2, \quad (39)$$

$$P_1(R_+, R_-, s) = 2(s^2 - R_-^2)(s^2 - R_+^2) [3s^4 + s^2(R_-^2 + R_+^2) - 5R_-^2 R_+^2], \quad (40)$$

$$P_2(R_+, R_-, s) = 3s^8 + 2s^6(R_-^2 + R_+^2) + 3s^4(R_-^4 + 4R_-^2 R_+^2 + R_+^4) - 30s^2 R_-^2 R_+^2 (R_-^2 + R_+^2) + 35R_-^4 R_+^4. \quad (41)$$

Inserting in Eq. (30) and using $\int d\hat{r} \int d\hat{r}' = 8\pi^2 \int_{R_-}^{R_+} \frac{s ds}{RR'}$, we obtain

$$\Pi^{(s)}(t, t', \omega) = \frac{\pi^2 \kappa^2 \rho_{\text{vac}}^2}{4 \cdot 9} \int_{-\infty}^t dt_N \Gamma(t_N) \int_{R_-}^{R_+} \frac{ds}{s^3} \sum_{i=0}^2 P_i \frac{j_i(\omega s)}{(\omega s)^i} e^{-I_{\text{tot}}(t, t', s)}. \quad (42)$$

For the two-bubble contribution (31), the vector $\mathbf{s} = \mathbf{1} + R'\hat{r}' - R\hat{r}$ is independent of \hat{r} and \hat{r}' . Changing the variable of integration \mathbf{l} to \mathbf{s} and using the result (32), the second line in (31) becomes

$$\sum_{i=0}^2 \int s^2 ds e^{-I_{\text{tot}}(t, t', s)} \frac{j_i(\omega s)}{(\omega s)^i} \int d\hat{s} \int d\hat{r} \int d\hat{r}' C_i. \quad (43)$$

The angular integrations with respect to \hat{r} and \hat{r}' are restrained by the Heaviside functions of Eq. (29), which give conditions on the cosines

$$\hat{r} \cdot \hat{s} \geq -\frac{s^2 + R^2 - (R + R_-)^2}{2sR} \equiv -c_M, \quad (44)$$

$$\hat{r}' \cdot \hat{s} \leq \frac{s^2 + R'^2 - (R' - R_-)^2}{2sR'} \equiv c'_M, \quad (45)$$

where we have defined $R_- = R(t, t') = \int_t^{t'} v_w(t'') dt''$ (notice that $R_- \neq R' - R$ in this case⁷). As shown in appendix B, the angular integrals vanish whenever c_M or c'_M is outside of the interval $[-1, +1]$.⁸ If the values of c_M and c'_M are both in the interval $[-1, +1]$, the integrals of C_0 and C_1 still vanish, while that of C_2 gives (see appendix B for details)

$$\int d\hat{s} \int d\hat{r} \int d\hat{r}' C_2 = 16\pi^3 (c_M - c_M^3)(c'_M - c_M'^3). \quad (46)$$

⁷While in the single-bubble case we have $R_- = R' - R = R(t, t')$, in the two-bubble case we have $R' - R \neq R(t, t')$ since the nucleation times are different in $R = R(t_N, t)$ and $R' = R(t'_N, t')$. In this case, the quantity $R' - R$ depends on the nucleation times, while $R_- \equiv R(t, t')$ does not.

⁸For instance, when $-c_M \geq 1$, the integral vanishes because there is no allowed range for the cosine $\hat{r} \cdot \hat{s}$. Physically, this situation occurs when the bubble of radius R is completely inside the bubble of radius R' in Fig. 1. On the other hand, when $-c_M \leq -1$, the whole range $-1 \leq \hat{r} \cdot \hat{s} \leq 1$ is allowed. This situation occurs when the separation between the two bubbles is such that they do not overlap, and the integral vanishes due to spherical symmetry.

The conditions $-1 \leq c_M, c'_M \leq 1$ are equivalent to

$$s \geq R_-, s \leq 2R' - R_-, s \leq 2R + R_-. \quad (47)$$

The latter two imply $s \leq \min\{2R' - R_-, 2R + R_-\} = R_+ - |R(t_N, t'_N)|$. Inserting the result (46) in Eq. (43), with c_M and c'_M given by (44)-(45), using the conditions (47), and finally inserting in Eq. (31), we obtain

$$\begin{aligned} \Pi^{(d)}(t, t', \omega) &= \frac{\pi^3}{4} \frac{\kappa^2 \rho_{\text{vac}}^2}{9} \int_{-\infty}^t dt_N \Gamma(t_N) \int_{-\infty}^{t'} dt'_N \Gamma(t'_N) \\ &\times \int_{R_-}^{R_+ - |R(t_N, t'_N)|} \frac{ds}{s^4} e^{-I_{\text{tot}}(t, t', s)} \frac{j_2(\omega s)}{(\omega s)^2} Q_+(s, R, R_-) Q_-(s, R', R_-). \end{aligned} \quad (48)$$

where the functions Q_{\pm} are given by

$$Q_+(s, R, R_-) = (s^2 - R_-^2) [(2R + R_-)^2 - s^2] [s^2 - R_-(2R + R_-)], \quad (49)$$

$$Q_-(s, R', R_-) = (s^2 - R_-^2) [(2R' - R_-)^2 - s^2] [s^2 + R_-(2R' - R_-)] \quad (50)$$

It can be seen that this result coincides with that of Ref. [37] for the case of an exponential nucleation rate and a constant wall velocity. We shall consider this case as well as other specific models elsewhere [57]. Our general expressions also seem to be in agreement with the expressions given in the different appendices of Ref. [39]. In any case, as shown in Appendix A, our method is equivalent to previous approaches.

4 The bulk flow model

The bulk flow model [39, 40] adapts the envelope approximation to take into account the fact that the bulk fluid motions do not disappear when bubbles collide. In this model, the energy is concentrated in thin fluid shells which form complete (overlapping) spheres. In each spherical shell, the surface energy density is not homogeneous, since the fluid is in contact with a bubble wall only in the uncollided regions of the bubble. The uncollided wall transfers an amount of energy to the fluid which is proportional to the bubble volume, and on the other hand the surface energy density decreases with the surface area, so it is given by Eq. (21). In a collided region, in contrast, the wall has disappeared and the fluid does not receive energy anymore. The fluid shell is assumed to move with the same velocity as the bubble wall (for consistency, the latter must be a constant). The energy density in that part of the fluid shell will thus be proportional to R_c^2/R^2 , where $R = v(t - t_N)$ is the bubble radius and $R_c = v(t_c - t_N)$ its value at the moment of collision t_c . The latter depends on the specific point on the bubble surface, which we represent by the unit vector \hat{r} . The stress-energy tensor for a bubble at time t is similar to that of the envelope approximation, Eqs. (18)-(19). In the present case we have

$$T_{ij} = \hat{r}_i \hat{r}_j \delta(r - R) \sigma(\hat{r}), \quad (51)$$

with

$$\sigma(\hat{r}) = \begin{cases} \sigma_u(t) & \text{for } t_c(\hat{r}) > t, \\ \sigma_c(t_c, t) & \text{for } t_c(\hat{r}) < t, \end{cases} \quad (52)$$

where $\sigma_u = (\kappa\rho_{\text{vac}}/3)R$ is the surface energy density at an uncollided point, while σ_c is the surface energy density at a collided point. The latter is given by

$$\sigma_c = \frac{\kappa\rho_{\text{vac}}}{3}R_c \times \frac{R_c^2}{R^2} \times D(t_c, t). \quad (53)$$

The first factor in (53) is the value of σ_u at the collision time of the given point. The second factor takes into account the scaling as R^{-2} , and the third factor is a damping function introduced to account for an additional energy loss [39]. We thus have

$$\sigma(\hat{r}) = \sigma_u(t) \begin{cases} 1 & \text{for } t_c(\hat{r}) > t, \\ \frac{(t_c - t_N)^3}{(t - t_N)^3} D(t_c, t) & \text{for } t_c(\hat{r}) < t, \end{cases} \quad (54)$$

Repeating the steps of Sec. 3, we readily arrive at expressions for $\Pi^{(s)}$ and $\Pi^{(d)}$ similar to Eqs. (22) and (23),

$$\Pi^{(s)}(t, t', \omega) = \int_{-\infty}^t dt_N \Gamma(t_N) f_+(t_N) R^2 R'^2 \int d\hat{r} \int d\hat{r}' e^{i\omega\hat{n}\cdot\mathbf{s}} \Lambda_{ij,kl} \hat{r}_i \hat{r}_j \hat{r}'_k \hat{r}'_l \langle \sigma\sigma' \rangle, \quad (55)$$

$$\begin{aligned} \Pi^{(d)}(t, t', \omega) &= \int_{-\infty}^t dt_N \Gamma(t_N) f_+(t_N) R^2 \int_{-\infty}^{t'} dt'_N \Gamma(t'_N) f_+(t'_N) R'^2 \\ &\times \int d^3l \int d\hat{r} \int d\hat{r}' e^{i\omega\hat{n}\cdot\mathbf{s}} \Lambda_{ij,kl} \hat{r}_i \hat{r}_j \hat{r}'_k \hat{r}'_l \langle \sigma\sigma' \rangle, \end{aligned} \quad (56)$$

where σ' is the surface energy density at angular position \hat{r}' on the bubble of radius $R' = v(t' - t'_N)$ at time t' (with $t'_N = t_N$ for the single-bubble case).

We must evaluate the average $\langle \sigma\sigma' \rangle$ at fixed times t, t' and fixed directions \hat{r}, \hat{r}' . The random variables here are the collision times $t_c(\hat{r}), t_c(\hat{r}')$ of each point. Notice that a given point on a bubble surface will eventually collide, and the probability for the collision time t_c does not depend on the time t (before or after t_c) at which we evaluate the average. This probability does depend on the knowledge of another point (on the same or a different bubble) being collided or not. Hence, we need to calculate the joint probability dP_{cc} that the collision time of the point at \hat{r} is in the interval $[t_c, t_c + dt_c]$ and the collision time of the point at \hat{r}' is in the interval $[t'_c, t'_c + dt'_c]$. This infinitesimal probability is related to the probability P_{cc} of both points having collided before the times t_c and t'_c through

$$dP_{cc} = \frac{\partial^2 P_{cc}}{\partial t_c \partial t'_c} dt_c dt'_c. \quad (57)$$

On the other hand, the probability P_{cc} is related to the probability P_{uu} that both points are uncollided, which is given by Eq. (26) for the single-bubble case and by Eq. (29) for

the two-bubble case. We have⁹

$$P_{cc} = 1 - P_u(t_c) - P_u(t'_c) + P_{uu}(t_c, t'_c, s_c), \quad (58)$$

where $P_u(t)$ is the probability that a single point on the bubble surface is uncollided at time t . The first three terms in (58) vanish when we take the second derivative in (57), and we have

$$\langle \sigma \sigma' \rangle = \int \sigma \sigma' dP_{cc} = \int_{t_N}^{\infty} \int_{t'_N}^{\infty} \sigma \sigma' \frac{\partial^2 P_{uu}}{\partial t_c \partial t'_c} dt_c dt'_c. \quad (59)$$

Integrating by parts and taking into account that $P_{uu} \rightarrow 0$ for $t_c \rightarrow \infty$ or $t'_c \rightarrow \infty$ (in which case one of the points is certainly collided) and that $\sigma(t_c = t_N) = \sigma'(t'_c = t'_N) = 0$ (corresponding to a collision as soon as the bubble nucleates), we obtain

$$\langle \sigma \sigma' \rangle = \int_{t_N}^{\infty} \int_{t'_N}^{\infty} \frac{\partial^2 (\sigma \sigma')}{\partial t_c \partial t'_c} P_{uu} dt_c dt'_c = \frac{\sigma_u \sigma'_u}{R'^3 R^3} \int_{t_N}^t dt_c \frac{\partial R_c^3 D}{\partial t_c} \int_{t'_N}^{t'} dt'_c \frac{\partial R'_c{}^3 D'}{\partial t'_c} P_{uu} \quad (60)$$

where we have used Eqs. (54). From now on, we shall consider for simplicity the case $D = 1$ (free propagation with no damping). Thus, we have

$$\langle \sigma \sigma' \rangle = (\kappa \rho_{\text{vac}})^2 v^2 \int_{t_N}^t dt_c \frac{R_c^2}{R^2} \int_{t'_N}^{t'} dt'_c \frac{R'_c{}^2}{R'^2} P_{uu}(t_c, t'_c, s_c). \quad (61)$$

Since Eqs. (55)-(56) are very similar to (22)-(23), we may proceed like in Sec. 3. In particular, the average over the direction of observation \hat{n} introduces the factor (32),

$$\sum_{i=0}^2 \frac{j_i(\omega s)}{(\omega s)^i} C_i(\hat{r} \cdot \hat{s}, \hat{r}' \cdot \hat{s}, \hat{r} \cdot \hat{r}'), \quad (62)$$

where the functions C_i are defined in Eqs. (34)-(36), and $\mathbf{s} = \mathbf{l} + R' \hat{r}' - R \hat{r}$ (with $\mathbf{l} = \mathbf{0}$ for the single-bubble case). The dependence on the vector \mathbf{s} comes from the factor $e^{i\omega \hat{n} \cdot \mathbf{s}}$ in (55)-(56). The main difference with the envelope approximation is that in that case we had

$$\langle \sigma \sigma' \rangle = \sigma_u \sigma'_u R^2 R'^2 \langle 1_S(\hat{r}) 1_{S'}(\hat{r}') \rangle = (\kappa \rho_{\text{vac}}/3)^2 R R' P_{uu}(t, t', s). \quad (63)$$

In the present case this expression must be replaced with (61), which depends on the vector $\mathbf{s}_c = \mathbf{l} + R'_c \hat{r}' - R_c \hat{r}$ joining the positions of the points at the collision times. The probability P_{uu} depends in this case on the quantity

$$I_{\cap}(t_c, t'_c, s_c) = \int_{-\infty}^{\min\{t_c, t'_c\}} dt'' \Gamma(t'') V_{\cap}(t'', t_c, t'_c, s_c). \quad (64)$$

⁹The normalization condition for probability implies that $P_{cc} = 1 - P_{uu} - P_{uc} - P_{cu}$, where P_{cu} and P_{uc} are the probabilities that only one of the points has collided before the corresponding time t_c or t'_c . These are given by $P_u(t_c) - P_{uu}$ and $P_u(t'_c) - P_{uu}$, where $P_u(t) = e^{-I(t)+I(t_N)}$ is the independent probability that a point on the bubble surface is uncollided at time t .

For the single-bubble contribution, the distance s is given by Eq. (37), and s_c has a similar expression in terms of $c = \hat{r} \cdot \hat{r}'$, which is the only independent angular variable in the integrand of (55). The variables s and s_c are thus related by

$$c = \frac{R^2 + R'^2 - s^2}{2RR'} = \frac{R_c^2 + R_c'^2 - s_c^2}{2R_c R_c'}, \quad (65)$$

and the angular integrals in (55) can be written in several forms,

$$\int d\hat{r} \int d\hat{r}' = 8\pi^2 \int_{-1}^{+1} dc = 8\pi^2 \int_{R_-}^{R_+} \frac{sd s}{RR'} = 8\pi^2 \int_{R_{c-}}^{R_{c+}} \frac{s_c ds_c}{R_c R_c'}, \quad (66)$$

with $R_{c\pm} = R'_c \pm R_c$. If we write $\hat{r} \cdot \hat{s}$ and $\hat{r}' \cdot \hat{s}$ in terms of c , Eq. (62) gives the expression (38). Then, if we choose s as the integration variable, like we did in Sec. 3, we obtain

$$\begin{aligned} \Pi^{(s)}(t, t', \omega) &= \frac{\pi^2}{4} (\kappa \rho_{\text{vac}})^2 v^2 \int_{-\infty}^t dt_N \Gamma(t_N) \int_{R_-}^{R_+} \frac{ds}{s^3} \sum_{i=0}^2 \frac{P_i(s, R, R')}{R^3 R'^3} \frac{j_i(\omega s)}{(\omega s)^i} \\ &\times \int_{t_N}^t dt_c R_c^2 \int_{t_N}^{t'} dt'_c R_c'^2 e^{-I_{\text{tot}}(t_c, t'_c, s_c)}. \end{aligned} \quad (67)$$

This expression is equivalent to Eq. (B.9) of Ref. [39].

For the two-bubble contribution, the integrations on \hat{r} and \hat{r}' are restrained by the Heaviside functions of Eq. (29) at the times t_c and t'_c , which give conditions like (44)-(45) but for the cosines $\hat{r} \cdot \hat{s}_c$ and $\hat{r}' \cdot \hat{s}_c$,

$$\hat{r} \cdot \hat{s}_c \geq -\frac{s_c^2 + R_c^2 - (R_c + R_{c-})^2}{2s_c R_c} \equiv -c_{Mc}, \quad (68)$$

$$\hat{r}' \cdot \hat{s}_c \leq \frac{s_c^2 + R_c'^2 - (R'_c - R_{c-})^2}{2s_c R_c'} \equiv c'_{Mc}, \quad (69)$$

where $R_{c-} = R(t_c, t'_c)$. In contrast, the quantities C_i in (62) depend on the cosines $\hat{r} \cdot \hat{s}$, $\hat{r}' \cdot \hat{s}$. The variables at the times t, t' are related to those at the collision times t_c, t'_c by

$$\mathbf{l} = \mathbf{s} - R'\hat{r}' + R\hat{r} = \mathbf{s}_c - R'_c\hat{r}' + R_c\hat{r}. \quad (70)$$

Using (70), we may change the variable of integration \mathbf{l} in Eq. (56) either to \mathbf{s} or to \mathbf{s}_c . The first choice leads to an expression which is equivalent to Eq. (B.18) of Ref. [39]. In this case it is convenient to define angular variables $c_r = \hat{r} \cdot \hat{s}$, $c_{r'} = \hat{r}' \cdot \hat{s}$ and the azimuth $\phi_{r'}$ like we did in appendix B,

$$\begin{aligned} \frac{\Pi^{(d)}}{\kappa^2 \rho_{\text{vac}}^2} &= 8\pi^2 v^2 \int_{-\infty}^t dt_N \Gamma(t_N) \int_{-\infty}^{t'} dt'_N \Gamma(t'_N) \int_{t_N}^t dt_c R_c^2 \int_{t'_N}^{t'} dt'_c R_c'^2 \\ &\times \int_0^\infty s^2 ds \sum_{i=0}^2 \frac{j_i(\omega s)}{(\omega s)^i} \int_{-1}^1 dc_r \int_{-1}^1 dc_{r'} \int_0^{2\pi} d\phi_{r'} C_i(c_r, c_{r'}, \hat{r} \cdot \hat{r}') e^{-I_{\text{tot}}(t_c, t'_c, s_c)} \\ &\times \Theta(\hat{r} \cdot \hat{s}_c + c_{Mc}) \Theta(c'_{Mc} - \hat{r}' \cdot \hat{s}_c). \end{aligned} \quad (71)$$

In the envelope approximation we made analytically the integrals $\int d\phi_{r'} C_i$. However, in this case the variable s_c also depends on $\phi_{r'}$.

Notice also that the Heaviside functions imposing the conditions (68)-(69) upon the integration domain are non-trivial in terms of the variables $c_r, c_{r'}$. A somewhat simpler expression is obtained if we use \mathbf{s}_c instead of \mathbf{s} as integration variable, since these restrictions can be implemented explicitly in the limits of integration. We proceed like we did in appendix B, but we define angular variables with respect to \mathbf{s}_c instead of \mathbf{s} , i.e., $c_{rc} = \hat{r} \cdot \hat{s}_c$, $c_{r'c} = \hat{r}' \cdot \hat{s}_c$, and the azimuth $\phi_{r'c}$ of \hat{r}' . We obtain

$$\begin{aligned} \frac{\Pi^{(d)}}{\kappa^2 \rho_{\text{vac}}^2} &= 8\pi^2 v^2 \int_{-\infty}^t dt_N \Gamma(t_N) \int_{-\infty}^{t'} dt'_N \Gamma(t'_N) \int_{t_N}^t dt_c R_c^2 \int_{t'_N}^{t'} dt'_c R_c'^2 \int_0^\infty ds_c s_c^2 e^{-I_{\text{tot}}(t_c, t'_c, s_c)} \\ &\times \int_{\max\{-c_{M_c}, -1\}}^1 dc_{rc} \int_{-1}^{\min\{c'_{M_c}, 1\}} dc_{r'c} \int_0^{2\pi} d\phi_{r'c} \sum_{i=0}^2 \frac{j_i(\omega s)}{(\omega s)^i} C_i(\hat{r} \cdot \hat{s}, \hat{r}' \cdot \hat{s}, \hat{r} \cdot \hat{r}'). \end{aligned} \quad (72)$$

Finally, the relation between the variables with and without the index c is obtained from Eq. (70),

$$s^2 = s_c^2 + \Delta R'^2 + \Delta R^2 + 2s_c \Delta R' (\hat{r}' \cdot \hat{s}_c) - 2s_c \Delta R (\hat{r} \cdot \hat{s}_c) - 2\Delta R' \Delta R (\hat{r} \cdot \hat{r}'), \quad (73)$$

$$\hat{r} \cdot \hat{s} = \frac{s_c \hat{r} \cdot \hat{s}_c + \Delta R' (\hat{r} \cdot \hat{r}') - \Delta R}{s}, \quad \hat{r}' \cdot \hat{s} = \frac{s_c \hat{r}' \cdot \hat{s}_c + \Delta R' - \Delta R (\hat{r} \cdot \hat{r}')}{s}, \quad (74)$$

where $\Delta R = R - R_c = v(t - t_c)$, $\Delta R' = R' - R'_c = v(t' - t'_c)$, and

$$\hat{r} \cdot \hat{r}' = s_{rc} s_{r'c} \cos \phi_{r'c} + c_{rc} c_{r'c}, \quad (75)$$

with $s_{rc}^2 = 1 - c_{rc}^2$, and $s_{r'c}^2 = 1 - c_{r'c}^2$.

We shall apply these expressions to specific phase transition models elsewhere. Here we shall focus on the case of non-spherical bubbles.

5 Wall deformations

We shall now adapt the derivation of $\Pi^{(s)}$ and $\Pi^{(d)}$ of Sec. 3 to the case of bubble walls which depart from the spherical shape.

5.1 A general wall shape

In general, the wall surface can be parametrized by a function of two variables. For instance, $\mathbf{r} = \mathbf{r}_w(\hat{r}) = r_w(\hat{r})\hat{r}$ in terms of the angles of the direction \hat{r} from the nucleation center. It is a good approximation to consider a field profile of the form [58]

$$\phi(\mathbf{r}) = \phi_0((\mathbf{r} - \mathbf{r}_w) \cdot \hat{n}_S), \quad (76)$$

where $\phi_0(x)$ is the bubble profile for the one-dimensional problem and \hat{n}_S is the normal to the surface. The function $\phi_0(x)$ varies only in a certain interval of length l_w (the wall

width) around $x = 0$ and takes approximately constant values outside this interval. If the implicit form of the surface is defined by an equation $F(\mathbf{r}) = 0$, we have $\hat{n}_S = \nabla F/|\nabla F|$. For instance, for a spherical bubble, the function F can be taken as $F(\mathbf{r}) = r - R$ (with $r = \sqrt{\mathbf{r}^2}$). This gives $\hat{n}_S = \nabla F = \hat{r}$ and $\phi(\mathbf{r}) = \phi_0(r - R)$, which is the form assumed in Sec. 3. For non-spherical bubbles, we write the wall position as $r_w = R + \zeta$. Then, for $F = r - R - \zeta$, we have $\nabla F = \hat{r} - \nabla\zeta$. Since ζ only varies in the angular directions, we have $\nabla\zeta \cdot \hat{r} = 0$ and $|\nabla F| = \sqrt{1 + (\nabla\zeta)^2}$. We thus obtain

$$\phi(r, \hat{r}, t) = \phi_0 \left(\frac{r - R - \zeta}{\sqrt{1 + (\nabla\zeta)^2}} \right), \quad (77)$$

where the time dependence is implicit in the undeformed wall position $R(t_N, t)$ as well as in the deformation $\zeta(\hat{r}, t)$.

Using Eq. (77) in $T_{ij} = \partial_i\phi\partial_j\phi$ we obtain

$$T_{ij} = \left[\phi'_0 \left(\frac{r - R - \zeta}{\sqrt{1 + (\nabla\zeta)^2}} \right) \right]^2 \frac{(\hat{r}_i - \partial_i\zeta)(\hat{r}_j - \partial_j\zeta) + \mathcal{O}(r - r_w)}{1 + (\nabla\zeta)^2}. \quad (78)$$

We do not write down the terms of order $r - r_w$, which vanish in the thin wall approximation. Like in Sec. 3, we make the approximation $[\phi'_0(x)]^2 = \sigma_0\delta(x)$, and the first factor in (78) becomes¹⁰

$$\sigma_0\delta \left(\frac{r - R - \zeta}{\sqrt{1 + (\nabla\zeta)^2}} \right) = \sigma_0\delta(r - R - \zeta) \sqrt{1 + (\nabla\zeta)^2}. \quad (79)$$

Like in the envelope approximation, we shall assume that the wall profile ϕ_0 just disappears in the intersections with other bubbles. Thus, we have¹¹

$$T_{ij} = \frac{(\hat{r}_i - \partial_i\zeta)(\hat{r}_j - \partial_j\zeta)}{\sqrt{1 + (\nabla\zeta)^2}} \sigma_0\delta(r - R - \zeta) 1_S(\hat{r}), \quad (80)$$

and its spatial Fourier transform, defined by Eq. (9), is given by

$$\tilde{T}_{ij}(t, \omega\hat{n}) = \sigma_0 R^2 \int d\hat{r} e^{-i\omega R\hat{n}\cdot\hat{r}} t_{ij} 1_S(\hat{r}), \quad (81)$$

where

$$t_{ij} = \frac{(1 + \zeta/R)^2}{\sqrt{1 + (\nabla\zeta)^2}} e^{-i\omega\zeta\hat{n}\cdot\hat{r}} (\hat{r}_i - \partial_i\zeta)(\hat{r}_j - \partial_j\zeta). \quad (82)$$

¹⁰Notice that Eq. (79) may be written as $\sigma_0\delta(F)|\nabla F| = \sigma_0\delta_S$, where δ_S is the surface delta, such that $\int \delta_S \varphi d^3x = \int_S \varphi dS$ for any test function φ .

¹¹To verify this result, let us consider the energy density of the scalar field in the static case, $T_{00} = \frac{1}{2}(\nabla\phi)^2 + V(\phi) = (\nabla\phi)^2$ (the last equality follows from the field equation inside the wall). Therefore, we have $T_{00} = \partial_i\phi\partial_i\phi = T_{ii}$. According to the result (80), we thus have $T_{00} = \sigma_0\delta(F)|\nabla F|1_S = \sigma_0\delta_S1_S$, as expected.

We shall again replace the parameter σ_0 by a varying quantity σ , so that we allow for the possibility that the surface energy density is not a constant. Inserting Eq. (81) into Eqs. (14) and (16), we obtain expressions similar to Eqs. (22)-(23),

$$\Pi^{(s)} = \int_{-\infty}^t dt_N \Gamma(t_N) f_+(t_N) \sigma R^2 \sigma' R'^2 \int d\hat{r} \int d\hat{r}' e^{i\omega\hat{n}\cdot\mathbf{s}} \Lambda_{ij,kl} \langle t_{ij} t_{kl}^* 1_S(\hat{r}) 1_{S'}(\hat{r}') \rangle, \quad (83)$$

$$\begin{aligned} \Pi^{(d)} &= \int_{-\infty}^t dt_N \Gamma(t_N) f_+(t_N) \sigma R^2 \int_{-\infty}^{t'} dt'_N \Gamma(t'_N) f_+(t'_N) \sigma' R'^2 \\ &\quad \times \int d^3l \int d\hat{r} \int d\hat{r}' e^{i\omega\hat{n}\cdot\mathbf{s}} \Lambda_{ij,kl} \langle t_{ij} t_{kl}^* 1_S(\hat{r}) 1_{S'}(\hat{r}') \rangle. \end{aligned} \quad (84)$$

Like in previous sections, a prime in a quantity means that it is evaluated at t' and \hat{r}' , and the definition of the vector \mathbf{s} is the same. Thus, t'_{kl} is given by Eq. (82) with R replaced by R' , \hat{r} by \hat{r}' , and ζ by $\zeta' \equiv \zeta(\hat{r}', t')$.

The ensemble average in Eqs. (83)-(84) involves a statistical treatment of the deformation ζ as well as that of the uncollided surfaces S and S' . In many cases, the dynamics of the wall deformation ζ will be independent of that of the uncollided surfaces. We expect this to be the case when the deformations originate from random perturbations. In such a case, the average separates,

$$\langle t_{ij} t_{kl}^* 1_S(\hat{r}) 1_{S'}(\hat{r}') \rangle = \langle t_{ij} t_{kl}^* \rangle \langle 1_S(\hat{r}) 1_{S'}(\hat{r}') \rangle = \langle t_{ij} t_{kl}^* \rangle P_{uu}(\hat{r}, \hat{r}') \quad (85)$$

where, assuming that the phase transition dynamics does not change significantly for deformed bubbles, P_{uu} is given by Eqs. (26) and (29). We thus obtain

$$\Pi^{(s)} = \int_{-\infty}^t dt_N \Gamma(t_N) \sigma R^2 \sigma' R'^2 \int d\hat{r} \int d\hat{r}' e^{i\omega\hat{n}\cdot\mathbf{s}} e^{-I_{\text{tot}}(t,t',s)} \Lambda_{ij,kl} \langle t_{ij} t_{kl}^* \rangle, \quad (86)$$

with $\mathbf{s} = R'\hat{r}' - R\hat{r}$, while for the two-bubble contribution the vector \mathbf{s} is independent of \hat{r} and \hat{r}' and we may change the variable of integration \mathbf{l} to \mathbf{s} like we did in Sec. 3. It is also reasonable to assume that there is no correlation between deformations produced in different bubbles, so in this case we have

$$\Pi^{(d)} = \int_{-\infty}^t dt_N \Gamma(t_N) \int_{-\infty}^{t'} dt'_N \Gamma(t'_N) \sigma R^2 \sigma' R'^2 \int d^3s e^{i\omega\hat{n}\cdot\mathbf{s}} e^{-I_{\text{tot}}} \int d\hat{r} \int d\hat{r}' \Lambda_{ij,kl} \langle t_{ij} \rangle \langle t_{kl}^* \rangle, \quad (87)$$

where the angular integrals are bound by the conditions (44)-(45).

5.2 Statistical properties of the deformations

The averages which remain to be evaluated in Eqs. (86)-(87) depend on the statistics of ζ . Assuming for simplicity a Gaussian probability distribution for the deformations, we only need to calculate the quantity $\langle \zeta \zeta' \rangle$ and its derivatives. For points on different bubbles we

assume that $\langle \zeta \zeta' \rangle = \langle \zeta \rangle \langle \zeta' \rangle = 0$, so we consider two points on a given bubble. Although the calculation cannot be done without considering a specific deformation mechanism, the general properties of these quantities are determined by the symmetry of the problem, since we consider deformations from a spherical shape.

The expectation value $\langle \zeta \zeta' \rangle$ depends on the times t, t' , as well as on the angular separation θ between \hat{r} and \hat{r}' . We thus write

$$\langle \zeta \zeta' \rangle \equiv \alpha(c, t, t'), \quad (88)$$

where $c \equiv \cos \theta \equiv \hat{r} \cdot \hat{r}'$, and we have¹²

$$\langle \zeta' \partial_i \zeta \rangle = \frac{\partial}{\partial x_i} \langle \zeta' \zeta \rangle = \frac{\hat{r}'_i - c \hat{r}_i}{R} \frac{\partial \alpha}{\partial c}. \quad (89)$$

Similarly,

$$\langle \zeta \partial_k \zeta' \rangle = \frac{\partial}{\partial x'_k} \langle \zeta \zeta' \rangle = \frac{\hat{r}_k - c \hat{r}'_k}{R'} \frac{\partial \alpha}{\partial c} \quad (90)$$

and

$$\langle \partial_i \zeta \partial_k \zeta' \rangle = \frac{\partial}{\partial x'_k} \frac{\partial}{\partial x_i} \langle \zeta \zeta' \rangle = \frac{\delta_{ik} - \hat{r}_i \hat{r}_k - \hat{r}'_i \hat{r}'_k + c \hat{r}_i \hat{r}'_k}{RR'} \frac{\partial \alpha}{\partial c} + \frac{(\hat{r}'_i - c \hat{r}_i)(\hat{r}_k - c \hat{r}'_k)}{RR'} \frac{\partial^2 \alpha}{\partial c^2}. \quad (91)$$

For $\hat{r}' \rightarrow \hat{r}$, we have $c \rightarrow 1$ and Eqs. (89)-(90) become

$$\langle \zeta' \partial_i \zeta \rangle = \langle \zeta \partial_k \zeta' \rangle = 0. \quad (92)$$

This was expected by symmetry, since $\nabla \zeta \perp \hat{r}$. Similarly, in this case Eq.(91) becomes

$$\langle \partial_i \zeta \partial_k \zeta' \rangle = \frac{\delta_{ik} - \hat{r}_i \hat{r}_k}{RR'} \frac{\partial \alpha}{\partial c}. \quad (93)$$

which is also expected by symmetry. In particular, at a given point on a bubble wall, i.e., for $\hat{r}' = \hat{r}$ and $t' = t$, we have

$$\langle \zeta^2 \rangle = \alpha_0(t), \quad \langle \zeta \partial_i \zeta \rangle = 0, \quad \langle \partial_i \zeta \partial_j \zeta \rangle = \beta_0(t) (\delta_{ij} - \hat{r}_i \hat{r}_j), \quad (94)$$

and $\langle (\nabla \zeta)^2 \rangle = 2\beta_0(t)$, where $\alpha_0(t) \equiv \alpha(1, t, t)$ and $\beta_0(t) \equiv R^{-2} \partial_c \alpha(1, t, t)$.

It is also useful to consider the expansion of the wall displacement in spherical harmonics,

$$\zeta(\hat{r}, t) = \sum_{l=0}^{\infty} \sum_{m=-l}^{+l} D_{lm}(t) Y_l^m(\hat{r}). \quad (95)$$

By symmetry, the correlator for the amplitude is of the form

$$\langle D_{lm}(t) D_{l'm'}(t')^* \rangle \equiv \delta_{ll'} \delta_{mm'} |D|_l^2(t, t'), \quad (96)$$

which yields (using the addition theorem of the spherical harmonics)

$$\alpha(c, t, t') = \langle \zeta(\hat{r}, t) \zeta(\hat{r}', t') \rangle = \sum_{l=0}^{\infty} \frac{2l+1}{4\pi} |D|_l^2(t, t') P_l(c), \quad (97)$$

where P_l are the Legendre polynomials.

¹²Using $\hat{r}_i = x_i/r$, $\partial(\hat{r} \cdot \hat{r}')/\partial x_i = r^{-1} [\hat{r}'_i - (\hat{r}' \cdot \hat{r}) \hat{r}_i]$.

5.3 Small deformations

If we expand the quantity t_{ij} in powers of ζ and $\partial_i\zeta$, we obtain $t_{ij} = t_{ij}^{(0)} + t_{ij}^{(1)} + \dots$, with

$$t_{ij}^{(0)} = \hat{r}_i \hat{r}_j e^{-i\omega\zeta \hat{n} \cdot \hat{r}}, \quad (98)$$

$$t_{ij}^{(1)} = \left[2\hat{r}_i \hat{r}_j \frac{\zeta}{R} - \hat{r}_i \partial_j \zeta - \hat{r}_j \partial_i \zeta \right] e^{-i\omega\zeta \hat{n} \cdot \hat{r}}, \quad (99)$$

$$t_{ij}^{(2)} = \left[\partial_i \zeta \partial_j \zeta + \hat{r}_i \hat{r}_j \left(\frac{\zeta^2}{R^2} - \frac{(\nabla\zeta)^2}{2} \right) - 2\frac{\zeta}{R} (\hat{r}_i \partial_j \zeta + \hat{r}_j \partial_i \zeta) \right] e^{-i\omega\zeta \hat{n} \cdot \hat{r}}, \quad (100)$$

and so on. We did not expand the exponential $e^{-i\omega\zeta \hat{n} \cdot \hat{r}}$, since $\omega\zeta$ may be large depending on ω . We shall consider for simplicity the case in which the length scale k_*^{-1} of the deformations is well separated from the typical bubble radius R_* . Therefore, we have $k_* R_* \gg 1$ and $\partial_i \zeta \sim k_* \zeta \gg \zeta/R$, which simplifies the expressions,

$$t_{ij}^{(0)} = \hat{r}_i \hat{r}_j e^{-i\omega\zeta \hat{n} \cdot \hat{r}}, \quad (101)$$

$$t_{ij}^{(1)} = -(\hat{r}_i \partial_j \zeta + \hat{r}_j \partial_i \zeta) e^{-i\omega\zeta \hat{n} \cdot \hat{r}}, \quad (102)$$

$$t_{ij}^{(2)} = [\partial_i \zeta \partial_j \zeta - \hat{r}_i \hat{r}_j (\nabla\zeta)^2 / 2] e^{-i\omega\zeta \hat{n} \cdot \hat{r}}. \quad (103)$$

We shall assume $k_* \zeta \lesssim 1$ and expand the product $t_{ij} t_{kl}^*$ to quadratic order in $\partial_i \zeta$, so we have

$$\langle t_{ij} t_{kl}^* \rangle = \langle t_{ij}^{(0)} t_{kl}^{(0)*} \rangle + \langle t_{ij}^{(0)} t_{kl}^{(1)*} \rangle + \langle t_{ij}^{(1)} t_{kl}^{(0)*} \rangle + \langle t_{ij}^{(0)} t_{kl}^{(2)*} \rangle + \langle t_{ij}^{(2)} t_{kl}^{(0)*} \rangle + \langle t_{ij}^{(1)} t_{kl}^{(1)*} \rangle. \quad (104)$$

In computing this quantity, we will have to deal with the average

$$\langle e^{i\omega \hat{n} \cdot (\zeta' \hat{r}' - \zeta \hat{r})} \rangle = \exp \left\{ -\frac{1}{2} \omega^2 [(\hat{n} \cdot \hat{r})^2 \langle \zeta^2 \rangle + (\hat{n} \cdot \hat{r}')^2 \langle \zeta'^2 \rangle - 2(\hat{n} \cdot \hat{r})(\hat{n} \cdot \hat{r}') \langle \zeta \zeta' \rangle] \right\}. \quad (105)$$

as well as

$$\langle \partial_i \zeta e^{i\omega \hat{n} \cdot (\zeta' \hat{r}' - \zeta \hat{r})} \rangle = i\omega (\hat{n} \cdot \hat{r}') \langle \partial_i \zeta \zeta' \rangle \langle e^{i\omega \hat{n} \cdot (\zeta' \hat{r}' - \zeta \hat{r})} \rangle, \quad (106)$$

$$\langle \partial_i \zeta \partial_j \zeta e^{i\omega \hat{n} \cdot (\zeta' \hat{r}' - \zeta \hat{r})} \rangle = [\langle \partial_i \zeta \partial_j \zeta \rangle - \omega^2 (\hat{n} \cdot \hat{r}')^2 \langle \zeta' \partial_i \zeta \rangle \langle \zeta' \partial_j \zeta \rangle] \langle e^{i\omega \hat{n} \cdot (\zeta' \hat{r}' - \zeta \hat{r})} \rangle, \quad (107)$$

$$\langle \partial_i \zeta \partial_k \zeta' e^{i\omega \hat{n} \cdot (\zeta' \hat{r}' - \zeta \hat{r})} \rangle = [\langle \partial_i \zeta \partial_k \zeta' \rangle - \omega^2 (\hat{n} \cdot \hat{r})(\hat{n} \cdot \hat{r}') \langle \zeta' \partial_i \zeta \rangle \langle \zeta \partial_k \zeta' \rangle] \langle e^{i\omega \hat{n} \cdot (\zeta' \hat{r}' - \zeta \hat{r})} \rangle \quad (108)$$

(and similar expressions interchanging $\hat{r} \leftrightarrow \hat{r}'$ and $\zeta \leftrightarrow \zeta'$). We derive these expressions in appendix C assuming Gaussian fluctuations. For the two-bubble contribution we have $\langle \zeta \zeta' \rangle = 0$, and several terms in these expressions vanish.

The zeroth order term in the expansion of $t_{ij} t_{kl}^*$ gives

$$\Lambda_{ij,kl} \langle t_{ij}^{(0)} t_{kl}^{(0)*} \rangle = (\Lambda_{ij,kl} \hat{r}_i \hat{r}_j \hat{r}'_k \hat{r}'_l) \langle e^{i\omega \hat{n} \cdot (\zeta' \hat{r}' - \zeta \hat{r})} \rangle. \quad (109)$$

The first factor, $\Lambda_{ij,kl} \hat{r}_i \hat{r}_j \hat{r}'_k \hat{r}'_l$, is given by Eq. (24). This factor alone would give the result of the bubble collision mechanism. However, it is modified by the average $\langle e^{i\omega \hat{n} \cdot (\zeta' \hat{r}' - \zeta \hat{r})} \rangle$. Since we consider small deformations, such that $\zeta \ll R_*$, for frequencies $\omega \sim R_*^{-1}$ Eq. (105)

gives $\langle e^{i\omega\hat{n}\cdot(\zeta'\hat{r}'-\zeta\hat{r})} \rangle \sim 1$. Therefore, Eq. (109) will reproduce the peak of the envelope approximation. If both the size and the amplitude of the relevant deformations are characterized by the length scale k_*^{-1} , we have $\langle \zeta^2 \rangle \sim k_*^{-2}$, and the argument of the exponential (105) will become of order 1 at the higher scale $\omega \sim k_*$.

Using the property $\Lambda_{ij,kl} = \Lambda_{ji,lk}$ and Eq. (106), the linear order terms in the expansion of $t_{ij}t_{kl}^*$ give

$$\Lambda_{ij,kl} \left(\langle t_{ij}^{(0)} t_{kl}^{*(1)} \rangle + \langle t_{ij}^{(1)} t_{kl}^{*(0)} \rangle \right) = 2i\omega\Lambda_{ij,kl} [(\hat{n} \cdot \hat{r})\hat{r}_i\hat{r}_j\hat{r}'_k\langle \zeta\partial_l\zeta' \rangle - (\hat{n} \cdot \hat{r}')\hat{r}_i\hat{r}'_j\hat{r}_k\langle \partial_j\zeta\zeta' \rangle] \langle e^{i\omega\hat{n}\cdot(\zeta'\hat{r}'-\zeta\hat{r})} \rangle \quad (110)$$

For the two-bubble contribution these terms vanish, since we have $\langle \zeta\partial_l\zeta' \rangle = \langle \zeta \rangle \langle \partial_l\zeta' \rangle = 0$ and the same for $\langle \partial_j\zeta\zeta' \rangle$. In the single-bubble case and for $k_*\zeta \lesssim 1$, these terms are small for $\omega \sim R_*^{-1}$, but are in principle of order 1 for $\omega \sim k_*$. However, one expects that short angular separations $\sim k_*^{-1}/R_*$ are relevant, and these averages are small for $\hat{r} \simeq \hat{r}'$, as shown in Eq. (90).

Let us now consider one of the three second-order terms contributing to $\langle t_{ij}t_{kl}^* \rangle$,

$$\Lambda_{ij,kl} \langle t_{ij}^{(2)} t_{kl}^{*(0)*} \rangle = \Lambda_{ij,kl} \hat{r}'_k\hat{r}'_l [\langle \partial_i\zeta\partial_j\zeta \rangle - \omega^2(\hat{n} \cdot \hat{r}')^2 \langle \zeta'\partial_i\zeta \rangle \langle \zeta'\partial_j\zeta \rangle] \langle e^{i\omega\hat{n}\cdot(\zeta'\hat{r}'-\zeta\hat{r})} \rangle - \Lambda_{ij,kl} \hat{r}_i\hat{r}_j\hat{r}'_k\hat{r}'_l \frac{1}{2} [\langle (\nabla\zeta)^2 \rangle - \omega^2(\hat{n} \cdot \hat{r}')^2 \langle \zeta'\nabla\zeta \rangle^2] \langle e^{i\omega\hat{n}\cdot(\zeta'\hat{r}'-\zeta\hat{r})} \rangle. \quad (111)$$

where we have used Eq. (107). The term $\langle t_{ij}^{(0)} t_{kl}^{*(2)*} \rangle$ is similar, with $\hat{r} \leftrightarrow \hat{r}'$ and $\zeta \leftrightarrow \zeta'$. We have not neglected the terms of order ζ^4 , since the accompanying factor ω^2 may be large. Nevertheless, as discussed above, for the two-bubble contribution the averages $\langle \zeta'\partial_i\zeta \rangle$ vanish, and in the single-bubble case they become small for deformations in a small length scale. Finally, for the term $\langle t_{ij}^{(1)} t_{kl}^{*(1)*} \rangle$ we have, using Eq. (108) and the property $\Lambda_{ij,kl} = \Lambda_{ji,lk}$,

$$\Lambda_{ij,kl} \langle t_{ij}^{(1)} t_{kl}^{*(1)*} \rangle = 2\Lambda_{ij,kl} [\hat{r}_j\hat{r}'_k\langle \partial_i\zeta\partial_l\zeta' \rangle + \hat{r}_j\hat{r}'_l\langle \partial_i\zeta\partial_k\zeta' \rangle] \langle e^{i\omega\hat{n}\cdot(\zeta'\hat{r}'-\zeta\hat{r})} \rangle + 2\omega^2(\hat{n} \cdot \hat{r})(\hat{n} \cdot \hat{r}')\Lambda_{ij,kl} [\hat{r}_j\hat{r}'_k\langle \zeta'\partial_i\zeta \rangle \langle \zeta\partial_l\zeta' \rangle + \hat{r}_j\hat{r}'_l\langle \zeta'\partial_i\zeta \rangle \langle \zeta\partial_k\zeta' \rangle] \langle e^{i\omega\hat{n}\cdot(\zeta'\hat{r}'-\zeta\hat{r})} \rangle. \quad (112)$$

This whole expression vanishes for the two-bubble case. For the single-bubble contribution, the terms which are of order $\omega^2\zeta^4$ (the whole last line), will be very small for a small length scale, due to small averages $\langle \zeta'\partial_i\zeta \rangle$.

5.4 Contributions to Π

To avoid long expressions, from now on we shall neglect the terms in (110)-(112) which are small when the characteristic length k_*^{-1} is such that $k_*R_* \gg 1$. Including them in a calculation (if necessary) is straightforward. Hence, we have

$$\Lambda_{ij,kl} \langle t_{ij}t_{kl}^* \rangle \simeq \Lambda_{ij,kl} \{ \hat{r}_i\hat{r}_j\hat{r}'_k\hat{r}'_l + \hat{r}'_k\hat{r}'_l\langle \partial_i\zeta\partial_j\zeta \rangle + \hat{r}_i\hat{r}_j\langle \partial_k\zeta'\partial_l\zeta' \rangle - \hat{r}_i\hat{r}_j\hat{r}'_k\hat{r}'_l \frac{1}{2} [\langle (\nabla\zeta)^2 \rangle + \langle (\nabla\zeta')^2 \rangle] + 2\hat{r}_j\hat{r}'_k\langle \partial_i\zeta\partial_l\zeta' \rangle + 2\hat{r}_j\hat{r}'_l\langle \partial_i\zeta\partial_k\zeta' \rangle \} \langle e^{i\omega\hat{n}\cdot(\zeta'\hat{r}'-\zeta\hat{r})} \rangle. \quad (113)$$

Inside the brackets, the first term is the contribution from $t_{ij}^{(0)} t_{kl}^{\prime(0)*}$, the terms in the second line are those from $t_{ij}^{(0)} t_{kl}^{\prime(2)*}$ and $t_{ij}^{(2)} t_{kl}^{\prime(0)*}$, and the last line contains the contribution from $t_{ij}^{(1)} t_{kl}^{\prime(1)*}$. We shall denote the corresponding contributions to Π by $\Pi^{(0,0)}$, $\Pi^{(0,2)}$, $\Pi^{(2,0)}$, and $\Pi^{(1,1)}$, respectively. Each of these terms separates into a single-bubble contribution corresponding to Eq. (86) and a two-bubble contribution corresponding to Eq. (87), except for $\Pi^{(1,1)}$, for which the two-bubble contribution vanishes. Like in the spherical case, the quantity σ varies during the phase transition, and is related to the energy released by each bubble. We shall assume again that it is given by Eq. (21). Thus, all the terms $\Pi^{(0,0)}$, $\Pi^{(0,2)}$, $\Pi^{(2,0)}$, $\Pi^{(1,1)}$ have a common factor

$$\sigma\sigma' = (\kappa\rho_{\text{vac}})^2 RR'/9. \quad (114)$$

According to Eq. (113), for the zeroth-order term Eqs. (86)-(87) coincide with Eqs. (30)-(31), except for the factor

$$\langle e^{i\omega\hat{n}\cdot(\zeta'\hat{r}'-\zeta\hat{r})} \rangle = \exp \left\{ -\frac{1}{2}\omega^2[\alpha_0(\hat{n}\cdot\hat{r})^2 + \alpha'_0(\hat{n}\cdot\hat{r}')^2 - 2\alpha(\hat{n}\cdot\hat{r})(\hat{n}\cdot\hat{r}')] \right\}, \quad (115)$$

where we use the notation $\alpha_0 \equiv \alpha_0(t)$, $\alpha'_0 = \alpha_0(t')$, $\alpha = \alpha(\theta, t, t')$. We have

$$\begin{aligned} \Pi^{(0,0)} = & \frac{\kappa^2 \rho_{\text{vac}}^2}{9} \left[\int_{-\infty}^t dt_N \Gamma(t_N) R^3 R'^3 \int d\hat{r} \int d\hat{r}' e^{-I_{\text{tot}}} e^{i\omega\hat{n}\cdot\mathbf{s}} A G^{(s)} \right. \\ & \left. + \int_{-\infty}^t dt_N \Gamma(t_N) \int_{-\infty}^{t'} dt'_N \Gamma(t'_N) R^3 R'^3 \int d^3s e^{-I_{\text{tot}}} e^{i\omega\hat{n}\cdot\mathbf{s}} \int d\hat{r} \int d\hat{r}' A G^{(d)} \right]. \quad (116) \end{aligned}$$

where $A = \Lambda_{ij,kl} \hat{r}_i \hat{r}_j \hat{r}'_k \hat{r}'_l$ and $G^{(s)}$ and $G^{(d)}$ are given by Eq. (115), only that for the latter we have $\alpha = 0$ [also, the angular integrals in the second line are constrained by the conditions (44)-(45)]. As anticipated, Eq. (116) is very similar to the bubble collision case (30)-(31). The main difference is the presence of the Gaussians in the integrand¹³. For the contribution $\Pi^{(0,2)} + \Pi^{(2,0)}$, we notice that the second line of Eq. (113), using the last of Eqs. (94) and taking into account that $\Lambda_{ij,kl} \delta_{ij} = 0$, gives

$$-2[\beta_0(t) + \beta_0(t')] \Lambda_{ij,kl} \hat{r}_i \hat{r}_j \hat{r}'_k \hat{r}'_l, \quad (117)$$

which is of the same form of the previous contribution, and we obtain

$$\Pi^{(0,0)} + \Pi^{(2,0)} + \Pi^{(0,2)} = [1 - 2\beta_0(t) - 2\beta_0(t')] \Pi^{(0,0)}, \quad (118)$$

On the other hand, for the contribution $\Pi^{(1,1)}$, we use Eq. (91) in the last line of Eq. (113) (in this case the two-bubble contribution vanishes). Using the property $\Lambda_{ij,kl} = \Lambda_{ji,lk}$, we obtain

$$\begin{aligned} \Lambda_{ij,kl} (2\hat{r}_j \hat{r}'_l \langle \partial_i \zeta \partial_k \zeta' \rangle + 2\hat{r}_j \hat{r}'_k \langle \partial_i \zeta \partial_l \zeta' \rangle) = \\ 2\Lambda_{ij,kl} \frac{\hat{r}_j (\hat{r}'_l \delta_{ik} + \hat{r}'_k \delta_{il}) - 2\hat{r}_i (\hat{r}_j \hat{r}'_k + \hat{r}'_j \hat{r}'_k) \hat{r}'_l + 2c\hat{r}_i \hat{r}_j \hat{r}'_k \hat{r}'_l \frac{\partial \alpha}{\partial c}}{RR'} \\ + 2\Lambda_{ij,kl} \frac{\hat{r}'_i \hat{r}_j (\hat{r}'_l \hat{r}_k + \hat{r}'_k \hat{r}_l) + 2c^2 \hat{r}_i \hat{r}_j \hat{r}'_k \hat{r}'_l - 2c\hat{r}_i (\hat{r}_j \hat{r}'_k + \hat{r}'_j \hat{r}'_k) \hat{r}'_l \frac{\partial^2 \alpha}{\partial c^2}}{RR'} \quad (119) \end{aligned}$$

¹³Notice that this extra dependence hinders any attempt to integrate out the vector \hat{n} like we did for the bubble collision mechanism.

In this case, besides the expression $A = \Lambda_{ij,kl} \hat{r}_i \hat{r}_j \hat{r}'_k \hat{r}'_l$, which is given by Eq. (24), we have also

$$A_1 = \Lambda_{ij,kl} (\hat{r}'_i \hat{r}_j \hat{r}_k \hat{r}'_l + \hat{r}'_i \hat{r}_j \hat{r}'_k \hat{r}_l) = [1 - (\hat{n} \cdot \hat{r})^2] [1 - (\hat{n} \cdot \hat{r}')^2], \quad (120)$$

$$A_2 = \Lambda_{ij,il} \hat{r}_j \hat{r}'_l + \Lambda_{ij,ki} \hat{r}_j \hat{r}'_k = 2 [\hat{r} \cdot \hat{r}' - (\hat{n} \cdot \hat{r})(\hat{n} \cdot \hat{r}')], \quad (121)$$

$$A_3 = \Lambda_{ij,kl} \hat{r}_j \hat{r}'_l (\hat{r}_i \hat{r}_k + \hat{r}'_i \hat{r}'_k) = \frac{1}{2} [(r \cdot r') - (\hat{n} \cdot r)(\hat{n} \cdot r')] [2 - (\hat{n} \cdot r)^2 - (\hat{n} \cdot r')^2]. \quad (122)$$

Thus, the contribution to Eq. (86) is of the form

$$\Pi^{(1,1)} = \frac{\kappa^2 \rho_{\text{vac}}^2}{9} \int_{-\infty}^t dt_N \Gamma(t_N) R^3 R'^3 \int d\hat{r} \int d\hat{r}' e^{-I_{\text{tot}}} e^{i\omega \hat{n} \cdot \mathbf{s}} G^{(s)} \frac{B \partial_c \alpha + C \partial_c^2 \alpha}{RR'}, \quad (123)$$

with $B = 2(A_2 - 2A_3 + 2cA)$ and $C = 2(A_1 + 2c^2A - 2cA_3)$.

6 A single deformation scale

The GW spectrum resulting from Eqs. (116), (118), (123) will depend on the dynamics of the deformations. For instance, in the case of hydrodynamic instabilities, the coupled equations for the wall deformations and the fluid perturbations must be considered. These quantities can be expanded in modes which diagonalize the equations. This has been done for a planar wall, in which case there is a range of unstable wavenumbers, and it is to be expected that the situation is similar in the spherical case. The most unstable wavelength is in general much shorter than the typical bubble radius by the end of the phase transition (see, e.g., [15]). The evolution of these perturbations beyond the linear order has not been studied, at least in this context¹⁴. One possibility is that the most unstable mode dominates, and we shall consider for simplicity a single length scale. If the instability persists in the nonlinear regime, this may lead to dendritic growth [60]. We will be more conservative and assume that the deformation grows up to an amplitude of the order of the deformation size k_*^{-1} .

6.1 The model

We could model such deformations by considering a single component in the expansion (97), i.e., setting $|D|_l^2(t, t') \propto \delta_{ll_*}$, where l_* is related to the deformation scale by $k_*^{-1} \sim R_*/l_*$. Assuming an average displacement $\sqrt{\langle \zeta^2 \rangle} \sim k_*^{-1}$, Eq. (97) gives

$$\frac{2l+1}{4\pi} |D|_l^2(t, t) = \left(\frac{a}{l_*}\right)^2 R^2 \delta_{ll_*}. \quad (124)$$

where a is a constant of order 1. For the unequal-time correlation function, we may assume for simplicity a maximal time correlation, $|D|_l(t, t') = \sqrt{|D|_l^2(t, t) |D|_l^2(t', t')}$, which gives

$$\frac{2l+1}{4\pi} |D|_l^2(t, t') = \left(\frac{a}{l_*}\right)^2 RR' \delta_{ll_*}. \quad (125)$$

¹⁴See e.g. [59] for similar instabilities in flames.

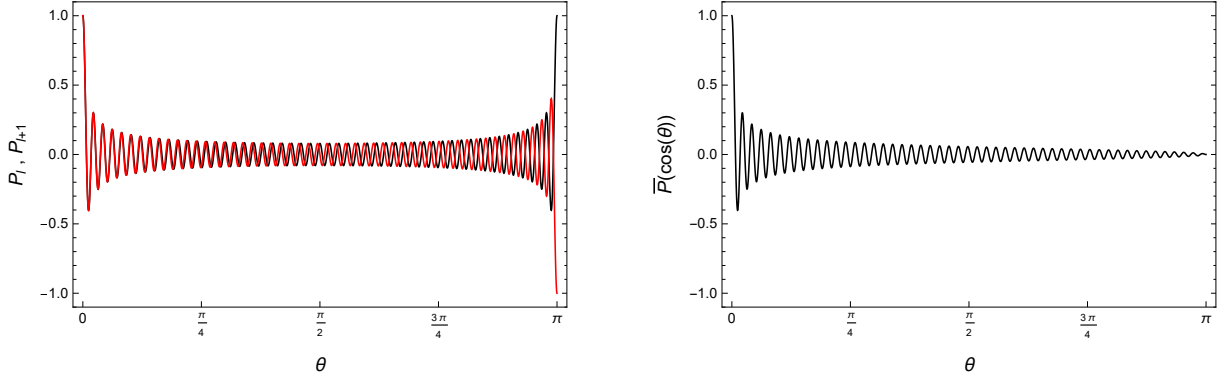


Figure 2: Two adjacent Legendre polynomials P_l (black) and P_{l+1} (red) with $l = 100$ and the function $\bar{P}(c)$ for $l_* = 100$.

Thus, Eq. (97) becomes $\alpha(c, t, t') = (a/l_*)^2 RR' P_{l_*}(c)$. The function $P_{l_*}(c)$ has a maximum at $c = 1$ (i.e., at $\theta = 0$), with $P_{l_*}(1) = 1$. For $0 < \theta < \pi$, this function oscillates with a smaller amplitude, but it has another extremum at $\theta = \pi$, with $P_{l_*}(-1) = (-1)^{l_*}$. This second peak of the correlation function for opposite points on the bubble wall is rather artificial. If we considered a displacement spectrum with many components l , the correlation function would actually vanish for $c = -1$ due to the superposition of alternating signs. We may reproduce this effect without departing significantly from the simple model (125) by considering two adjacent components,

$$\alpha(c, t, t') = \frac{a^2}{l_*^2} RR' \frac{P_{l_*}(c) + P_{l_*+1}(c)}{2} \equiv \frac{a^2}{l_*^2} RR' \bar{P}(c). \quad (126)$$

Figure 2 shows the form of the function $\bar{P}(c)$ for $l_* = 100$.

We shall consider the case $l_* \gg 1$, so that we have $k_*^{-1} \ll R_*$. Thus, Eq. (126) gives $\langle \zeta^2 \rangle = \alpha(1, t, t) \sim (R_*/l_*)^2 \ll 1$, which justifies the expansion of Eq. (82) in powers of ζ/R and the approximations used in Eqs. (101)-(103). On the other hand, the derivatives of α are much larger. In particular, taking into account that $P'_l(1) = l(l+1)/2$, we have $\beta_0 = R^{-2} \partial_c \alpha(1, t, t) \simeq a^2/2$. Since $\langle (\nabla \zeta)^2 \rangle = 2\beta_0(t) \simeq a^2$, the constant a must be smaller than 1 so that the expansion of Eq. (82) in powers of $(\nabla \zeta)^2$ is valid. A well known asymptotic approximation for the Legendre polynomials for large l_* , namely, $P_{l_*}(\cos \theta) = \sqrt{\frac{2}{\pi l_* \sin \theta}} \cos \left[\left(l_* + \frac{1}{2} \right) \theta - \frac{\pi}{4} \right]$, gives

$$\bar{P}(\cos \theta) \simeq \sqrt{\frac{2}{\pi l_* \sin \theta}} \cos \frac{\theta}{2} \cos \left(l_* \theta - \frac{\pi}{4} \right), \quad (127)$$

which is a very good approximation for $\theta \geq l_*^{-1}$. For $\theta < l_*^{-1}$, we may use the Taylor expansion $1 - \frac{1}{4} l_*^2 \theta^2 + \frac{1}{64} l_*^4 \theta^4$ (where we have also made the approximation of large l_*).

We will also consider for simplicity a constant velocity v and a simultaneous nucleation, i.e., $\Gamma(t) = n_* \delta(t - t_*)$, where n_* is the number density of bubbles. We use this parameter

to define the characteristic bubble size by $R_* = n_*^{-1/3}$, and we define a dimensionless spectrum¹⁵

$$\Delta(R_*\omega) = \frac{3R_*^{-2}}{8\pi G\kappa^2\rho_{\text{vac}}^2} \frac{d\rho_{GW}}{d\ln\omega}(\omega). \quad (128)$$

Inserting Eqs. (116) and (123) in Eq. (3), we obtain the contributions to Δ . With the change of variables $t, t' \rightarrow t - t_*, t' - t_*$ we have

$$\begin{aligned} \Delta^{(0,0)} &= \frac{\omega^3}{3\pi R_*^5} \int_0^\infty dt \int_t^\infty dt' \cos[\omega(t' - t)] (RR')^3 \\ &\times \left[\int d\hat{r} \int d\hat{r}' e^{-I_{\text{tot}}} e^{i\omega\hat{n}\cdot\mathbf{s}} A G^{(s)} + R_*^{-3} \int d^3s e^{-I_{\text{tot}}} e^{i\omega\hat{n}\cdot\mathbf{s}} \int d\hat{r} \int d\hat{r}' A G^{(d)} \right], \end{aligned} \quad (129)$$

where $G^{(s,d)}$ denote the Gaussian (115) for the single-bubble or two-bubble case,

$$G^{(s)} = \exp \left\{ -\frac{\omega^2 a^2}{2l_*^2} [(\hat{n} \cdot \hat{r})^2 R^2 + (\hat{n} \cdot \hat{r}')^2 R'^2 - 2(\hat{n} \cdot \hat{r})(\hat{n} \cdot \hat{r}') RR' \bar{P}(c)] \right\}, \quad (130)$$

$$G^{(d)} = \exp \left\{ -\frac{\omega^2 a^2}{2l_*^2} [(\hat{n} \cdot \hat{r})^2 R^2 + (\hat{n} \cdot \hat{r}')^2 R'^2] \right\}. \quad (131)$$

In terms of $R_\pm = vt_\pm = v(t' \pm t)$ we have

$$I_{\text{tot}} = \frac{\pi}{12R_*^3} [2R_+^3 + 3sR_+^2 - s^3 + 3s^{-1}(R_+ + s)^2 R_-^2], \quad (132)$$

with $s^2 = R^2 + R'^2 - 2RR'c$ for the single-bubble term, while \mathbf{s} is an independent variable for the two-bubble term. In the latter, the integrals are restrained by the conditions

$$\hat{r} \cdot \mathbf{s} \geq -\frac{s^2 - R_+R_-}{R_+ - R_-}, \quad \hat{r}' \cdot \mathbf{s} \leq \frac{s^2 + R_+R_-}{R_+ + R_-}. \quad (133)$$

On the other hand, for this model Eq. (118) gives

$$\Delta^{(0,0)} + \Delta^{(2,0)} + \Delta^{(0,2)} = (1 - 2a^2) \Delta^{(0,0)}. \quad (134)$$

If we integrate first \hat{r}' , putting \hat{r} in the z axis and \hat{n} in the xz plane, we have

$$\hat{r}' \cdot \hat{r} = \cos\theta, \quad \hat{n} \cdot \hat{r} = \cos\chi, \quad \hat{n} \cdot \hat{r}' = \cos\chi \cos\theta + \sin\chi \cos\phi \sin\theta, \quad (135)$$

where θ is the angle between \hat{r}' and \hat{r} , ϕ is the azimuthal angle of \hat{r}' , and χ is the angle between \hat{r} and \hat{n} (see Fig. 4). Thus, the angular integrations become $\int d\hat{r} \int d\hat{r}' = 2\pi \int_{-1}^{+1} dc_\chi \int_{-1}^{+1} dc \int_0^{2\pi} d\phi$. Using the abbreviated notation $c_\chi = \cos\chi$, $s_\chi = \sin\chi$, $c_\phi = \cos\phi$ (as well as $c = \cos\theta$), we have

$$A = \frac{1}{2} s_\chi^2 \left[2(cs_\chi - c_\chi c_\phi \sqrt{1 - c^2})^2 + (c_\chi c + s_\chi c_\phi \sqrt{1 - c^2})^2 - 1 \right]. \quad (136)$$

¹⁵A very similar function was defined in Refs. [36,37] for an exponential nucleation rate $\Gamma = \Gamma_* e^{\beta(t-t_*)}$, with R_*^{-2} replaced by β^2 .

Finally, Eq. (123) gives (changing variables $t, t' \rightarrow R, R'$)

$$\begin{aligned} \Delta^{(1,1)} = \frac{a^2 \omega^3 R_*^{-2}}{3\pi l_*^2 v^2} \int_0^\infty dR \int_R^\infty dR' \cos(\omega R_- / v) R^3 R'^3 \int_{-1}^{+1} dc_\chi \int_0^{2\pi} d\phi \\ \times \int_{-1}^{+1} dc e^{-I_{\text{tot}}} e^{i\omega \hat{n} \cdot \mathbf{s}} G^{(s)} (B \partial_c \bar{P} + C \partial_c^2 \bar{P}), \end{aligned} \quad (137)$$

with

$$\begin{aligned} B = 2 \left[2(1 - s_\chi^2 c_\phi^2) s_\chi^2 c^3 + (2c_\phi^2 - 1) s_\chi^4 c + c_\chi s_\chi c_\phi (s_\chi^2 c_\phi^2 c^2 - c_\chi^2 c^2 - c_\chi^2 - s_\chi^2 c_\phi^2) \sqrt{1 - c^2} \right], \\ C = 2 \left[2(s_\chi^2 c_\phi^2 - 1) s_\chi^2 c^2 - (s_\chi^2 c_\phi^2 - c_\chi^2) c_\chi s_\chi c_\phi c \sqrt{1 - c^2} + s_\chi^2 (1 - s_\chi^2 c_\phi^2) \right] (1 - c^2), \end{aligned} \quad (138)$$

and $\hat{n} \cdot \mathbf{s} = (R' \cos \theta - R) c_\chi + R' s_\chi c_\phi \sin \theta$.

In order to deal with the function $\bar{P}(\cos \theta)$ in the exponent of Eq. (130), we notice that, for large l_* , this function takes order-1 values only in a very small interval of length l_*^{-1} close to $\theta = 0$, while for most of the interval $0 < \theta < \pi$ it oscillates with an amplitude of order $l_*^{-1/2}$. Therefore, we can write

$$G^{(s)} \simeq G^{(d)} \left[1 + (\omega a / l_*)^2 c_\chi (c_\chi \cos \theta + s_\chi \cos \phi \sin \theta) R R' \bar{P}(c) \right], \quad (139)$$

This approximation is valid for values of ω up to $\omega \sim l_* / R_*$, while for $\omega \gg l_* / R_*$ the quantity Δ will be negligible anyway. According to the approximation (127), the function \bar{P} in the second term of Eq. (139) combines with $\partial_c \bar{P}$ and $\partial_c^2 \bar{P}$ in Eq. (137) to form an oscillating function with frequency $2l_*$. Therefore, the calculation of this contribution is similar to that of the first term. We shall ignore this $\mathcal{O}(l_*^{-1/2})$ correction for simplicity, so from now on we assume

$$G^{(s)} \simeq G^{(d)} = \exp \left\{ -\frac{1}{2} \left(\frac{\omega a}{l_*} \right)^2 \left[c_\chi^2 R^2 + (c_\chi \cos \theta + s_\chi \cos \phi \sin \theta)^2 R'^2 \right] \right\} \equiv G. \quad (140)$$

6.2 Contributions to Δ

We shall consider separately different spectral ranges. For $\omega \sim R_*^{-1}$, the argument of the exponential (140) is of order l_*^{-2} , and we use the approximation $G^{(s)} \simeq G^{(d)} \simeq 1$. Therefore, $\Delta^{(0,0)}$ gives the same result of the envelope approximation, Δ_{env} . In this case the term $\Delta^{(1,1)}$ will be suppressed with respect to the other contributions. This can be seen, e.g., by integrating by parts the derivatives ∂_c in Eq. (137). Indeed, these derivatives only produce factors of order 1. In particular, the derivatives of $e^{i\omega \hat{n} \cdot \mathbf{s}}$ produce factors of order $\omega R_* \sim 1$ (which will be important for higher frequencies). Since $\bar{P} \sim 1$, the contribution (137) is suppressed by the factor l_*^{-2} . Besides the function $\bar{P}(c)$ oscillates with frequency l_* , which also causes a suppression of the integral. Hence, in this frequency scale the spectrum is given by

$$\Delta = \Delta^{(0,0)} + \Delta^{(2,0)} + \Delta^{(0,2)} = (1 - 2a^2) \Pi_{\text{env}}. \quad (141)$$

Let us now consider the case $\omega \sim l_*/R_*$. In this case the range of variation in R, R' of the Gaussian (140) becomes of order R_* , so the presence of this function in the integrand begins to be noticeable. Nevertheless, the function $e^{-I_{\text{tot}}}$ falls more quickly, since we have, roughly, $G \sim e^{-a^2(R/R_*)^2}$ and $e^{-I_{\text{tot}}} \sim e^{-I(t)} \sim e^{-\frac{4\pi}{3}(R/R_*)^3}$. Therefore, the contribution (129) will not depart significantly from the result of the envelope approximation until higher ω , where the function $G \sim \exp[-(a\omega R_*/l_*)^2(R/R_*)^2]$ will reduce the effective support for the integration. We shall then assume that, at $\omega \sim l_*/R_*$, the contribution $\Delta^{(0,0)}$ is still roughly given by the envelope approximation, and concentrate in the contribution $\Pi^{(1,1)}$, which has a different behavior.

In the case $\omega \sim k_* \sim l_*/R_*$, if we integrate by parts the second line of Eq. (137) there are terms which are not suppressed, namely, those containing derivatives of the exponential $e^{i\omega\hat{n}\cdot\mathbf{s}}$. In fact, the dominant term is the one containing two derivatives, $\partial_c^2 e^{i\omega\hat{n}\cdot\mathbf{s}}$. Considering only this contribution, we obtain

$$\begin{aligned} \Delta^{(1,1)} = & -\frac{a^2 v^2 \omega^5}{3\pi R_*^5 l_*^2} \int_0^\infty dR' \int_0^{R'} dR \cos(v^{-1}\omega R_-) (RR')^3 R'^2 \\ & \times \int_{-1}^{+1} dc_\chi \int_0^{2\pi} d\phi \int_{-1}^{+1} dc e^{-I_{\text{tot}}} G e^{i\omega\hat{n}\cdot\mathbf{s}} C \left(c_n - s_n c_\phi \frac{\cos\theta}{\sin\theta} \right)^2 \bar{P}(c), \end{aligned} \quad (142)$$

The function $e^{-I_{\text{tot}}}$ sets an effective integration range for R and R' of order R_* . For $\omega \sim l_*/R_*$, the function G is smooth in this range, while the functions $\cos(v^{-1}\omega R_-)$ and $e^{i\omega\hat{n}\cdot\mathbf{s}}$ have strong oscillations. Similarly, according to Eq. (127), the function $\bar{P}(\cos\theta)$ oscillates with a very high frequency l_* . We shall avoid the difficult oscillatory integrals by using approximations such as the stationary phase approximation and integrating by parts recursively to obtain an expansion in powers of ω^{-1} . The calculation is described in appendix D. We obtain

$$\Delta^{(1,1)}(R_*\omega) = \frac{4a^2 l_*^3}{3(R_*\omega)^5} \exp\left(-\frac{4\pi l_*^3}{3(R_*\omega)^3}\right). \quad (143)$$

This estimation is in principle only valid for $R_*\omega \sim l_*$, but it falls quickly from its peak at $\omega_p = (4\pi/5)^{1/3} l_*/R_*$. Around the maximum, the error of the approximation is of order $1/\sqrt{l_*}$.

6.3 The spectrum

For $\omega \sim R_*$ the GW spectrum is given by Eq. (141). To estimate the spectrum from the envelope approximation we shall use the results of Ref. [37]. That calculation was done for an exponential nucleation rate $\Gamma = \Gamma_* e^{\beta(t-t_*)}$, while we are considering a simultaneous nucleation. Nevertheless, the two models have been compared by relating their characteristic length scales (see, e.g., [56, 61, 62]). Indeed, for the exponential rate the GW spectrum is determined by the parameters v and β . For this model, the final bubble separation is given by $R_* = (8\pi)^{1/3} v/\beta$, and we shall use this relation to write β as a function of R_* . In Ref. [37], a dimensionless spectrum Δ_β was used. The definition of

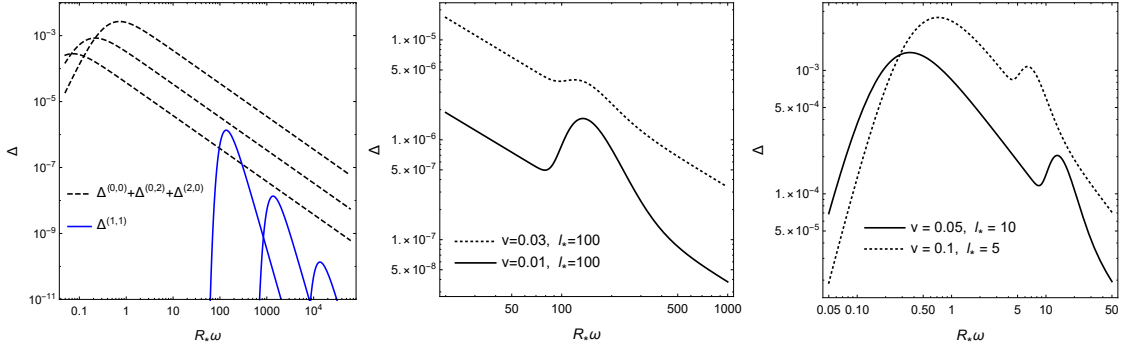


Figure 3: Left panel: The contribution $\Delta^{(0,0)} + \Delta^{(2,0)} + \Delta^{(0,2)}$ for different velocities (from top to bottom, $v = 0.1, 0.03, 0.01$), and the contribution $\Delta^{(1,1)}$ for different values of l_* (from top to bottom, $l_* = 100, 1000, 10000$). Central panel: The sum of these contributions for two sets of the parameters. Right panel: Extrapolation to smaller values of l_* .

Δ_β is similar to that of Eq. (128), with R_* replaced by β^{-1} . Hence, we have the relation $\Delta(R_*\omega) = (R_*\beta)^{-2}\Delta_\beta(R_*\omega/(R_*\beta))$, with a conversion factor $R_*\beta = (8\pi)^{1/3}v$. A fitting formula was provided in [37] for the spectrum,

$$\Delta_\beta = \Delta_p \left[c_l \left(\frac{\omega_p}{\omega} \right)^3 + (1 - c_l - c_h) \frac{\omega_p}{\omega} + c_h \frac{\omega}{\omega_p} \right]^{-1}, \quad (144)$$

with $c_l = 0.064$, $c_h = 0.48$, and

$$\Delta_p = 0.48v^3/(1 + 5.3v^2 + 5v^4), \quad \omega_p/\beta = 2\pi \times 0.35/(1 + 0.069v + 0.69v^4). \quad (145)$$

In the left panel of Fig. 3 we show the curves of $(1 - 2a^2)\Delta_{\text{env}}$ for a few velocities (dashed lines). All the curves correspond to $a = 0.5$. For a given value of l_* , we have argued that this approximation for the contribution $\Delta^{(0,0)} + \Delta^{(2,0)} + \Delta^{(0,2)}$ should be valid up to $wR_* \sim l_*$. The contribution $\Delta^{(1,1)}$, given by Eq. (143) is also shown in the left panel of Fig. 3 for a few values of l_* . We see that the relative amplitude of the two contributions depends on the values of v and l_* . In the central panel we show the sum of these contributions for two combinations of these parameters. The bump at $\omega \sim l_*/R_*$ will be more pronounced for lower wall velocities and for smaller l_* .

We remark that our perturbative calculation has severely limited the intensity of the effect, since we needed to consider wall deformations with amplitude $\zeta \sim aR_*/l_*$, with $a < 1$. For $a > 1$ the effect will be certainly stronger. Besides, we used the approximation $l_* \gg 1$ to neglect several terms and we approximated the integrals to lowest order in $1/l_*$. In particular, the latter have errors of order $l_*^{-1/2}$, so the value $l_* = 100$ is already in the limit of validity of our estimations. However, the only physical restriction on the deformation scale is $k_*^{-1} < R_*$, i.e., $l_* > 1$. Let us thus end with a speculation on the effect of deformations on a scale which is closer to the bubble size. For that aim we just extrapolate our results to $l_* = 10$ and $l_* = 5$ in the right panel of Fig. 3.

7 Conclusions

We have discussed a general method for calculating the gravitational waves generated by the motion of thin bubble walls or thin fluid shells in a cosmological phase transition. The main difference with previous approaches is in the calculation of the correlator of the energy-momentum tensor $\langle T_{ij}(t, \mathbf{x})T_{kl}(t', \mathbf{x}') \rangle$, although our approach takes ingredients from previous works [35, 37]. In the technique introduced in Ref. [37], two arbitrary space-time points t, \mathbf{x} and t', \mathbf{x}' are considered, and then the probability that bubbles are nucleated in the “past light cones” of these points is analyzed in order to determine whether a thin wall is present at each of the events. In contrast, we directly consider points on the bubble walls, which we assume from the beginning to be infinitely thin, and we write T_{ij} as a sum over bubbles, as done in the approach introduced in Ref. [35]. On the other hand, in the latter work the phase transition is simulated by nucleating bubbles in a certain volume and following their evolution, while we calculate the correlator statistically from the nucleation rate $\Gamma(t)$, like in Ref. [37].

We have exemplified the method by applying it to the bubble-collision mechanism in the envelope approximation and to the bulk flow model. The fact that we follow the motion of points on bubble walls makes our method geometrically clear, while the statistical treatment facilitates analytic calculations. Thus, for these cases we have seen that some steps of the derivations are much simpler than in other approaches. For instance, the decomposition of T_{ij} into a sum of individual bubble contributions gives naturally a single-bubble contribution and a two-bubble contribution to $\langle T_{ij}T_{kl} \rangle$. Furthermore, since we consider from the beginning only the uncollided parts of a bubble surface, the breaking of the spherical symmetry in the single-bubble case is also clear. Our method also allowed us to arrive more directly to the general expressions for the bulk flow model than it was done in the original work [39] with the approach of Ref. [37], and we have also discussed alternative expressions.

We have also considered the case of bubble walls which are deformed from the spherical configuration. In this case, our general expression for the GW spectrum contains the correlator of the surface deformation at two points on a wall, $\langle \zeta(t, \hat{r})\zeta(t', \hat{r}') \rangle$, which depends on the specific dynamics of the deformations. This result can be applied, e.g., to the case of inhomogeneous wall velocities due to inhomogeneous reheating during the phase transition or to the case of wall corrugations arising from hydrodynamic instabilities of deflagrations. For small enough deformations, the general expressions can be expanded perturbatively, which simplifies considerably the calculations. The lowest order is the result of the envelope approximation. However, the corrections introduce a suppression factor to this component, as well as a contribution which becomes relevant at frequencies associated to the deformation dynamics.

As a simple application we have modeled a wall deformation spectrum which peaks at a single length scale k_*^{-1} . This introduces a peak in the GW spectrum at $\omega \sim k_*$, which is always at a higher scale than that corresponding to the bubble size, R_*^{-1} . The perturbative expansion requires considering $\zeta \lesssim R_*$ as well as $k_*\zeta \lesssim 1$, which implies that, within this approximation, it is impossible to obtain an important effect for very

large k_* . We do have a clear difference (a second peak) from the GW spectrum of the bubble-collision mechanism for $k_* \lesssim 100/R_*$. We remark that this is a conservative estimate, and the effect may be quite larger. The wall deformations may range from scales of order R_* (from bubble interactions) to several orders of magnitude smaller (from instabilities). In the first case, the spectrum will have a bump close to the peak of the traditional GW generation mechanisms (bubble collisions, sound waves, turbulence). For the electroweak phase transition, this effect could be detected by LISA. In the case of much smaller deformations, there will be a peak at $\omega \gg R_*^{-1}$, which could be observed by other future detectors such as BBO [63], DECIGO [64], ET [65], or AEDGE [66].

Acknowledgments

This work was supported by CONICET grant PIP 11220130100172 and Universidad Nacional de Mar del Plata, grant EXA999/20.

A Gravitational waves from a stochastic source

Consider the gravitational waves emitted by a volume V in a direction \hat{n} . If this radiation is observed in the wave zone, the total energy per solid angle and per unit frequency interval is given by [67]

$$\frac{dE}{d \ln \omega d\Omega} = 2G\omega^3 \Lambda_{ij,kl}(\hat{n}) T_{ij}(\omega, \hat{n})^* T_{kl}(\omega, \hat{n}), \quad (146)$$

where

$$T_{ij}(\omega, \hat{n}) = \int_{-\infty}^{\infty} \frac{dt}{2\pi} e^{i\omega t} \int_V d^3x e^{-i\omega \hat{n} \cdot \mathbf{x}} T_{ij}(t, \mathbf{x}). \quad (147)$$

In Refs. [35, 36], T_{ij} is written as a sum over bubbles and the phase transition is simulated with a certain number of bubbles. We shall also use the explicit decomposition $T_{ij} = \sum_n T_{ij}^{(n)}$, but, since the contribution of many bubbles makes the phase transition a stochastic source, we shall consider the average on a statistical ensemble. Due to the homogeneity and isotropy of this source, the energy radiated in direction \hat{n} does not actually depend on \hat{n} . Therefore, integrating the angular variables in Eq. (146) only gives a factor of 4π . Thus, considering a large volume V , we may write

$$\frac{d\rho_{GW}}{d \ln \omega} = \frac{4\pi}{V} \left\langle \frac{dE}{d \ln \omega d\Omega} \right\rangle, \quad (148)$$

and using Eqs. (146-147) we obtain

$$\frac{d\rho_{GW}}{d \ln \omega} = \frac{2G\omega^3}{\pi} \int_{-\infty}^{\infty} dt \int_{-\infty}^{\infty} dt' e^{i\omega(t-t')} \Pi(t, t', \omega), \quad (149)$$

where Π is the quantity defined in Eq. (4),

$$\Pi = \frac{1}{V} \int_V d^3x \int_V d^3x' e^{-i\omega\hat{n}\cdot(\mathbf{x}-\mathbf{x}')} \langle \Lambda_{ij,kl}(\hat{n}) T_{ij}(t, \mathbf{x}) T_{kl}(t', \mathbf{x}') \rangle. \quad (150)$$

It is convenient to find an alternative expression, in which the times t and t' have a definite time ordering. For that aim, we shall first show that Π is real, does not depend on \hat{n} , and satisfies $\Pi(t, t', \omega) = \Pi(t', t, \omega)$. These properties follow from those of the quantity

$$\langle \Lambda TT \rangle \equiv \langle \Lambda_{ij,kl}(\hat{n}) T_{ij}(t, \mathbf{x}) T_{kl}(t', \mathbf{x}') \rangle. \quad (151)$$

By translation symmetry, this quantity depends only on the difference $\mathbf{r} = \mathbf{x} - \mathbf{x}'$. Hence, one of the integrals in Eq. (150) gives a factor of V ,

$$\Pi = \int_V d^3r e^{-i\omega\hat{n}\cdot\mathbf{r}} \langle \Lambda TT \rangle(t, t', \mathbf{r}) \quad (152)$$

By rotation symmetry, $\langle \Lambda TT \rangle$ only depends on r and on $\cos \chi = \hat{r} \cdot \hat{n}$. For very large V , we have

$$\Pi = 2\pi \int_0^\infty dr r^2 \int_0^\pi d\chi \sin \chi e^{-i\omega r \cos \chi} \langle \Lambda TT \rangle(t, t', r, \cos \chi). \quad (153)$$

The dependence on \hat{n} disappears upon integration on χ .

Using the properties $\Lambda_{ij,kl}(\hat{n}) = \Lambda_{kl,ij}(\hat{n})$ and $\Lambda_{ij,kl}(-\hat{n}) = \Lambda_{ij,kl}(\hat{n})$, we have

$$\langle \Lambda TT \rangle(t, t', r, \hat{n} \cdot \hat{r}) = \langle \Lambda TT \rangle(t', t, r, -\hat{n} \cdot \hat{r}) = \langle \Lambda TT \rangle(t', t, r, \hat{n} \cdot \hat{r}). \quad (154)$$

This implies that $\Pi(t, t', \omega) = \Pi(t', t, \omega)$. Besides, $\langle \Lambda TT \rangle$ is real, and Eq. (154) shows that it is even in $\cos \chi$, so we can write

$$\Pi = 2\pi \int_0^\infty dr r^2 \int_{-1}^{+1} du \cos(\omega r u) \langle \Lambda TT \rangle(t, t', r, u), \quad (155)$$

which is real. Since ρ_{GW} and Π are real, we may take the real part of the expression (149), so that the exponential becomes a cosine. Then, using the symmetry of Π under $t \leftrightarrow t'$ to write $\int_{-\infty}^{+\infty} dt' = 2 \int_t^\infty dt'$, we obtain Eq. (3),

$$\frac{d\rho_{GW}}{d \ln \omega} = \frac{4G\omega^3}{\pi} \int_{-\infty}^\infty dt \int_t^\infty dt' \cos[\omega(t-t')] \Pi(t, t', \omega). \quad (156)$$

Since our starting point, Eq. (146), was the same as in Refs. [35, 36], and the contribution of many bubbles makes the phase transition a stochastic source, our treatment should be equivalent. It is not difficult to see also the equivalence of Eq. (156) with the one used in Refs. [37, 38]. There, the evolution of the metric perturbations $h_{ij}(t, \mathbf{k})$ is solved with the Green function method, which relates h_{ij} with $\Pi_{ij}(t, \mathbf{k}) = \Lambda_{ij,kl} T_{kl}(t, \mathbf{k})$. Then, the energy density of the stochastic background of GWs is obtained from $\langle \dot{h}_{ij}(t, \mathbf{k}) \dot{h}_{ij}^*(t, \mathbf{q}) \rangle$. In this approach, the quantity Π is defined through the unequal-time correlator

$$\langle \Pi_{ij}(t, \mathbf{k}) \Pi_{ij}^*(t', \mathbf{q}) \rangle = (2\pi)^3 \delta^{(3)}(\mathbf{k} - \mathbf{q}) \Pi(t, t', k). \quad (157)$$

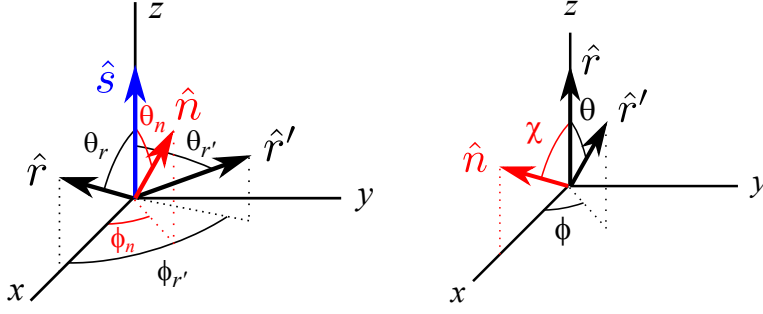


Figure 4: The unit vectors \hat{r} , \hat{r}' , \hat{s} , \hat{n} and their angles for two different orientations of the axes.

Since $T_{kl}(t, \mathbf{k}) = \int d^3x e^{i\mathbf{k}\cdot\mathbf{x}} T_{kl}(t, \mathbf{x})$, and taking into account the projector property of $\Lambda_{ij,kl}$, namely, $\Lambda_{ij,kl}\Lambda_{ij,mn} = \Lambda_{kl,mn}$, we have

$$\langle \Pi_{ij}(t, \mathbf{k}) \Pi_{ij}^*(t', \mathbf{q}) \rangle = \int d^3x e^{i\mathbf{k}\cdot\mathbf{x}} \int d^3x' e^{i\mathbf{q}\cdot\mathbf{x}'} \langle \Lambda T T \rangle(t, t', \mathbf{x} - \mathbf{x}'). \quad (158)$$

The translation invariance gives a delta function, and comparing with (157) we obtain

$$\Pi(t, t', k) = \int d^3r e^{i\mathbf{k}\cdot\mathbf{r}} \langle \Lambda T T \rangle(t, t', \mathbf{r}) \quad (159)$$

(cf. Eqs.(18-19) of Ref. [37]). Writing $\mathbf{k} = \omega\hat{n}$, this expression essentially coincides with our Eq. (152).

B Averaging the direction of observation

In this appendix we calculate the angular average

$$\frac{1}{4\pi} \int d\hat{n} e^{i\omega\hat{n}\cdot\mathbf{s}} \Lambda_{ij,kl}(\hat{n}) \hat{r}_i \hat{r}_j \hat{r}'_k \hat{r}'_l, \quad (160)$$

and then the angular integrals in Eqs. (30) and (31).

The quantity $\Lambda_{ij,kl}(\hat{n}) \hat{r}_i \hat{r}_j \hat{r}'_k \hat{r}'_l$, which is given by Eq. (24), contains angles of \hat{n} with \hat{r} and \hat{r}' . To perform the integral over \hat{n} , it is convenient to put the z axis in the direction of the vector \mathbf{s} , so that the exponential $e^{i\omega\hat{n}\cdot\mathbf{s}}$ depends on a single angle. We also put the vector \hat{r} in the xz plane (see Fig. 4), which simplifies a little the expressions. We thus write $\hat{s} = (0, 0, 1)$, $\hat{r} = (s_r, 0, c_r)$, with $c_r \equiv \cos\theta_r$ and $s_r^2 = 1 - c_r^2$, $\hat{r}' = (s_{r'} \cos\phi_{r'}, s_{r'} \sin\phi_{r'}, c_{r'})$, with $c_{r'} = \cos\theta_{r'}$ and $s_{r'}^2 = 1 - c_{r'}^2$, and $\hat{n} = (s_n \cos\phi_n, s_n \sin\phi_n, c_n)$, with $c_n = \cos\theta_n$ and $s_n^2 = 1 - c_n^2$. Thus, we have $\hat{n} \cdot \hat{s} = c_n$, $d\hat{n} = dc_n d\phi_n$ and the exponential becomes $e^{i\omega s c_n}$. On the other hand, the quantity $\Lambda_{ij,kl}(\hat{n}) \hat{r}_i \hat{r}_j \hat{r}'_k \hat{r}'_l$ contains the scalar products

$$\hat{n} \cdot \hat{r} = s_r s_n \cos\phi_n + c_r c_n. \quad (161)$$

$$\hat{n} \cdot \hat{r}' = s_{r'} s_n \cos\phi_{r'} \cos\phi_n + s_{r'} s_n \sin\phi_{r'} \sin\phi_n + c_{r'} c_n. \quad (162)$$

Inserting Eqs. (161-162) in Eq. (24), the expression becomes rather cumbersome. Nevertheless, the integral with respect to ϕ_n is straightforward, since we only have a few powers of $\cos \phi_n$ and $\sin \phi_n$. After integrating this angle, we obtain a simple polynomial in c_n , of the form $A + Bc_n^2 + Cc_n^4$. The integrals $\int_{-1}^1 dc_n e^{i\omega s c_n} c_n^k$ are readily evaluated. The result can be written in terms of the spherical Bessel functions (33). We obtain

$$\frac{1}{4\pi} \int d\hat{n} e^{i\omega \hat{n} \cdot \mathbf{s}} \Lambda_{ij,kl}(\hat{n}) \hat{r}_i \hat{r}_j \hat{r}'_k \hat{r}'_l = C_0 j_0(\omega s) + C_1 \frac{j_1(\omega s)}{\omega s} + C_2 \frac{j_2(\omega s)}{(\omega s)^2}. \quad (163)$$

The coefficients C_i depend on c_r , $c_{r'}$, $\phi_{r'}$, and $\hat{r} \cdot \hat{r}'$. The latter two variables are related by

$$\hat{r} \cdot \hat{r}' = s_r s_{r'} \cos \phi_{r'} + c_r c_{r'}. \quad (164)$$

We can eliminate $\phi_{r'}$, and we obtain

$$\begin{aligned} C_0 &= -\frac{1}{2} + \frac{c_r^2}{2} + \frac{c_{r'}^2}{2} + \frac{c_r^2 c_{r'}^2}{2} - 2c_r c_{r'} (\hat{r} \cdot \hat{r}') + (\hat{r} \cdot \hat{r}')^2, \\ C_1 &= 1 - c_r^2 - c_{r'}^2 - 5c_r^2 c_{r'}^2 + 8c_r c_{r'} (\hat{r} \cdot \hat{r}') - 2(\hat{r} \cdot \hat{r}')^2, \\ C_2 &= \frac{1}{2} - \frac{5}{2}c_r^2 - \frac{5}{2}c_{r'}^2 + \frac{35}{2}c_r^2 c_{r'}^2 - 10c_r c_{r'} (\hat{r} \cdot \hat{r}') + (\hat{r} \cdot \hat{r}')^2. \end{aligned} \quad (165)$$

Using $c_r = \hat{r} \cdot \hat{s}$, $c_{r'} = \hat{r}' \cdot \hat{s}$, we obtain the expressions given in Eqs. (34)-(36).

For the single-bubble case, \hat{s} is related to \hat{r} and \hat{r}' through $s\hat{s} = R'\hat{r}' - R\hat{r}$, so we have

$$\hat{r} \cdot \hat{s} = (R'\hat{r}' \cdot \hat{r}' - R)/s, \quad \hat{r}' \cdot \hat{s} = (R' - R\hat{r} \cdot \hat{r}')/s, \quad (166)$$

and Eq. (163) depends on a single cosine, which is related to s by

$$\hat{r} \cdot \hat{r}' = (R'^2 + R^2 - s^2)/2RR'. \quad (167)$$

Thus, we obtain

$$\frac{1}{4\pi} \int d\hat{n} e^{i\omega \hat{n} \cdot \mathbf{s}} (\Lambda_{ij,kl} \hat{r}_i \hat{r}_j \hat{r}'_k \hat{r}'_l) = \frac{1}{32R'^2 R^2 s^4} \sum_{i=0}^2 P_i \frac{j_i(\omega s)}{(\omega s)^i}, \quad (168)$$

with

$$P_0 = [(R' - R)^2 - s^2]^2 [(R' + R)^2 - s^2]^2, \quad (169)$$

$$P_1 = 2 [(R' - R)^2 - s^2] [(R' + R)^2 - s^2] [3s^4 + 2s^2(R'^2 + R^2) - 5(R^2 - R'^2)^2], \quad (170)$$

$$\begin{aligned} P_2 &= 3s^8 + 4s^6(R'^2 + R^2) + 6s^4(3R'^4 + 2R'^2 R^2 + 3R^4) \\ &\quad - 60s^2(R^2 - R'^2)^2(R'^2 + R^2) + 35(R^2 - R'^2)^4. \end{aligned} \quad (171)$$

Since this result depends only on the cosine $c = \hat{r} \cdot \hat{r}'$, the angular integrals in Eq. (30) can be written as $\int d\hat{r} \int d\hat{r}' = 8\pi^2 \int_{-1}^{+1} dc = 8\pi^2 \int_{R_-}^{R_+} \frac{s ds}{RR'}$.

For the two-bubble case, the vector \mathbf{s} is independent of \hat{r} and \hat{r}' , and the angular integrals $\int d\hat{s} \int d\hat{r} \int d\hat{r}'$ in Eq. (43) are straightforward. We only need to take into account

the restrictions (44)-(45), $-c_M \leq \hat{r} \cdot \hat{s} \leq 1$ and $-1 \leq \hat{r}' \cdot \hat{s} \leq c'_M$. For the integral over \hat{r}' we may put \hat{s} in the z axis and \hat{r} in the xz plane, like in Fig. 4 (where the variable \hat{n} is already integrated). Thus, the quantities C_i in Eqs. (165) depend on $\phi_{r'}$ through Eq. (164), and the integration on this variable is trivial. We obtain

$$\int_0^{2\pi} d\phi_{r'} C_0 = 0, \quad \int_0^{2\pi} d\phi_{r'} C_1 = 0, \quad \int_0^{2\pi} d\phi_{r'} C_2 = 2\pi (1 - 3c_r^2) (1 - 3c_{r'}^2). \quad (172)$$

The result depends only on $c_r = \hat{r} \cdot \hat{s}$, $c_{r'} = \hat{r}' \cdot \hat{s}$, and the integral on the azimuth ϕ_r gives a factor of 2π . The integrals on the polar angles are also trivial and we only have to take into account the conditions $-c_M \leq c_r \leq 1$ and $-1 \leq c_{r'} \leq c'_M$. If both limits c_M, c'_M are in the range $[-1, 1]$, we have

$$\int_{-c_M}^1 dc_r (1 - 3c_r^2) \int_{-1}^{c'_M} dc_{r'} (1 - 3c_{r'}^2) = (c_M - c_M^3)(c'_M - c_M'^3). \quad (173)$$

Otherwise, the result vanishes. Finally, the integral over \hat{s} gives a factor of 4π .

C Averaging the deformations

We consider the average

$$\left\langle e^{i(a\zeta + b\zeta')} \right\rangle \equiv G(a, b). \quad (174)$$

The function G is the characteristic function for the two variables ζ, ζ' . We shall assume a normal distribution with $\langle \zeta \rangle = \langle \zeta' \rangle = 0$. Therefore, we have¹⁶

$$G(a, b) = \exp \left[-\frac{a^2 \langle \zeta^2 \rangle + b^2 \langle \zeta'^2 \rangle + 2ab \langle \zeta \zeta' \rangle}{2} \right]. \quad (175)$$

Any expectation value can be derived from the characteristic functional for the entire stochastic process¹⁷. However, for our purposes it suffices with the characteristic function for a few points. For instance, applying $-i\partial/\partial x_i$ to (174)-(175)¹⁸ and taking into account that, by symmetry, $\langle \zeta^2 \rangle$ does not depend on the point on the bubble wall, and $\langle \zeta \partial_i \zeta \rangle = 0$, we obtain

$$\left\langle \partial_i \zeta e^{i(a\zeta + b\zeta')} \right\rangle = ib \langle \partial_i \zeta \zeta' \rangle G. \quad (176)$$

Applying $-i\partial/\partial x'_k$ to the latter, we obtain

$$\left\langle \partial_i \zeta \partial_k \zeta' e^{i(a\zeta + b\zeta')} \right\rangle = [\langle \partial_i \zeta \partial_k \zeta' \rangle - ab \langle \zeta' \partial_i \zeta \rangle \langle \zeta \partial_k \zeta' \rangle] G. \quad (177)$$

¹⁶See, e.g., [68].

¹⁷Namely, $G[a] = \langle \exp [i \int a(\hat{r}, t) \zeta(\hat{r}, t) d\hat{r} dt] \rangle$.

¹⁸Notice that, for these derivations, we may consider the variables a, b as independent of x_i or x'_k . Later we may evaluate the result at $a = -\omega \hat{n} \cdot \hat{r}$, $b = \omega \hat{n} \cdot \hat{r}'$.

If we consider a third point $\zeta'' = \zeta(\hat{r}'', t'')$, the generating function $G(a, b, c)$ is the trivial generalization of Eqs. (174)-(175). We thus obtain the generalization of Eq. (176),

$$\left\langle \partial_i \zeta e^{i(a\zeta + b\zeta' + c\zeta'')} \right\rangle = i [b \langle \zeta' \partial_i \zeta \rangle + c \langle \zeta'' \partial_i \zeta \rangle] G(a, b, c), \quad (178)$$

and, applying $-i\partial/\partial x_j''$, we have

$$\left\langle \partial_i \zeta \partial_j \zeta'' e^{i(a\zeta + b\zeta' + c\zeta'')} \right\rangle = \langle \partial_j \zeta'' \partial_i \zeta \rangle \varphi - (b \langle \zeta' \partial_i \zeta \rangle + c \langle \zeta'' \partial_i \zeta \rangle) (a \langle \zeta \partial_j \zeta'' \rangle + b \langle \zeta' \partial_j \zeta'' \rangle) G. \quad (179)$$

Evaluating in $c = 0$ and $\zeta'' = \zeta$, we obtain

$$\left\langle \partial_i \zeta \partial_j \zeta e^{i(a\zeta + b\zeta')} \right\rangle = [\langle \partial_i \zeta \partial_j \zeta \rangle - b^2 \langle \zeta' \partial_i \zeta \rangle \langle \zeta' \partial_j \zeta \rangle] G. \quad (180)$$

D Approximations for $\Delta^{(1,1)}$

We shall estimate the integrals in Eq. (142), which we write in the form

$$\begin{aligned} \Delta^{(1,1)} = & -\frac{a^2 v^2 \omega^5}{6\pi R_*^5 l_*^2} \int_0^\infty dR_+ \int_0^{R_+} dR_- \cos(v^{-1} \omega R_-) \left(\frac{R_+^2 - R_-^2}{4} \right)^3 \left(\frac{R_+ + R_-}{2} \right)^2 \\ & \times \int_{-1}^{+1} dc_\chi \int_0^{2\pi} d\phi \int_{-1}^{+1} dc e^{-I_{\text{tot}}(s,t,t')} G e^{i\omega \hat{n} \cdot \mathbf{s}} (\sin \theta c_\chi - \cos \theta s_\chi c_\phi)^2 \frac{C}{\sin^2 \theta} \bar{P}(c), \end{aligned} \quad (181)$$

where

$$G = \exp \left\{ -\frac{1}{2} \frac{\omega^2 a^2}{l_*^2} \left[c_\chi^2 \left(\frac{R_+ - R_-}{2} \right)^2 + (c_\chi c + s_\chi \cos \phi \sin \theta)^2 \left(\frac{R_+ + R_-}{2} \right)^2 \right] \right\}, \quad (182)$$

$$\frac{C}{\sin^2 \theta} = 2 \left[2 (s_\chi^2 c_\phi^2 - 1) s_\chi^2 c^2 - (s_\chi^2 c_\phi^2 - c_\chi^2) c_\chi s_\chi c_\phi c \sin \theta + s_\chi^2 (1 - s_\chi^2 c_\phi^2) \right] \quad (183)$$

and

$$e^{i\omega \hat{n} \cdot \mathbf{s}} = \exp \left\{ i\omega \left[(c_\chi c + s_\chi c_\phi \sin \theta - c_\chi) \frac{R_+}{2} + (c_\chi c + s_\chi c_\phi \sin \theta + c_\chi) \frac{R_-}{2} \right] \right\}. \quad (184)$$

We first approximate the integral with respect to R_- . We have an integral of the form

$$I_{R_-} = \int_0^{R_+} dR_- (e^{i\omega y_+ R_-} + e^{i\omega y_- R_-}) F(R_-), \quad (185)$$

with $y_\pm = v^{-1} + \frac{1}{2} (c_\chi \cos \theta + s_\chi c_\phi \sin \theta + c_\chi)$ and $F(R_-) = \left(\frac{R_+^2 - R_-^2}{4} \right)^3 \left(\frac{R_+ + R_-}{2} \right)^2 e^{-I_{\text{tot}}} G$. Integrating by parts twice, we obtain

$$I_{R_-} = \frac{v^2}{i\omega} \frac{\psi}{1 - \frac{v^2}{4} \psi^2} F(0) - \frac{2v^2}{\omega^2} \frac{1 + \frac{v^2}{4} \psi^2}{(1 - \frac{v^2}{4} \psi^2)^2} \frac{\partial F}{\partial R_-}(0) + \mathcal{O} \left(\frac{1}{\omega^3} \right), \quad (186)$$

where $\psi = c_\chi \cos \theta + s_\chi c_\phi \sin \theta + c_\chi$. This variable will vanish upon angular integration. This is why we kept the second order term in Eq. (186). Denoting $\bar{R} = R_+/2$, we have $F(0) = \bar{R}^8 e^{-I_{\text{tot}}} G$ and

$$F'(0) = \bar{R}^7 \left\{ 1 - \frac{1}{2} \frac{\omega^2 a^2}{l_*^2} \bar{R}^2 [(c_\chi \cos \theta + s_\chi \cos \phi \sin \theta)^2 - c_\chi^2] \right\} e^{-I_{\text{tot}}} G, \quad (187)$$

where now we have

$$I_{\text{tot}} = \frac{\pi \bar{R}^3}{6 \bar{R}_*^3} \left[8 + 6\sqrt{2(1-c)} - \sqrt{2}(1-c)^{3/2} \right] \quad (188)$$

and

$$G = \exp \left\{ -\frac{1}{2} \frac{\omega^2 a^2}{l_*^2} [c_\chi^2 + (c_\chi \cos \theta + s_\chi \cos \phi \sin \theta)^2] \bar{R}^2 \right\} \quad (189)$$

Now we will approximate the integral with respect to ϕ . We have an integral of the form

$$I_\phi = \int_0^{2\pi} d\phi e^{i\omega s_\chi \sin \theta \bar{R} \cos \phi} H(\phi), \quad (190)$$

where $H = \frac{C}{\sin^2 \theta} (\sin \theta c_\chi - \cos \theta s_\chi c_\phi)^2 I_{R_-}$. For large ω , we can use the stationary phase approximation. Since the integrand is periodic in ϕ we shift the integration interval to $[-\pi/2, 3\pi/2]$, where the cosine has stationary points at $\phi = 0$ and $\phi = \pi$. We obtain

$$I_\phi = e^{i\omega \bar{R} s_\chi \sin \theta} H_- + e^{-i\omega \bar{R} s_\chi \sin \theta} H_+, \quad (191)$$

where

$$H_- = e^{-i\pi/4} \sqrt{\frac{2\pi}{\omega \bar{R} s_\chi \sin \theta}} H(0), \quad H_+ = e^{+i\pi/4} \sqrt{\frac{2\pi}{\omega \bar{R} s_\chi \sin \theta}} H(\pi). \quad (192)$$

Next, we estimate the integral with respect to $c_\chi = \cos \chi$. The exponentials in (191) combine with the remaining exponentials in (184) and give exponents of the form $i\omega \bar{R}[(\cos(\chi \mp \theta) - \cos \chi)]$. For χ and θ in the interval $[0, \pi]$, there is only one stationary point for each case, at $\chi_\mp = \pi/2 \pm \theta/2$, and we obtain

$$\begin{aligned} \int_0^\pi d\chi \sin \chi e^{i\omega \bar{R}[\cos(\chi \mp \theta) - \cos \chi]} H_\mp(\chi) &= \sqrt{\frac{\pi}{\omega \bar{R} \sin \frac{\theta}{2}}} e^{\pm i\omega \bar{R} 2 \sin \frac{\theta}{2} \mp i\frac{\pi}{4}} \cos \frac{\theta}{2} H_\mp(\chi_\mp = \frac{\pi}{2} \pm \frac{\theta}{2}) \\ &= \mp i \frac{2\pi}{\omega \bar{R}} e^{\pm i\omega \bar{R} 2 \sin(\theta/2)} \sin(\theta/2) \cos^4(\theta/2) I_{R_-}. \end{aligned} \quad (193)$$

For these values of χ we have $c_\chi = \cos \chi_\mp = \mp \sin(\theta/2)$, $s_\chi = \sin \chi_\mp = \cos(\theta/2)$, which gives $\psi = 0$, so Eq. (186) becomes $I_{R_-} = -(2v^2/\omega^2) \partial_{R_-} F(0)$. Replacing all these results in Eq. (181), we have so far

$$\Delta^{(1,1)} = \frac{8a^2 \omega^2}{3\bar{R}_*^5 l_*^2} \int_0^\infty d\bar{R} \bar{R}^6 \int_0^\pi d\theta \sin \theta \sin \frac{\theta}{2} \cos^4 \frac{\theta}{2} e^{-I_{\text{tot}}} G \sin[\omega \bar{R} 2 \sin(\theta/2)] \bar{P}(c), \quad (194)$$

with $G = \exp[-(\omega a/l_*)^2 \sin^2(\theta/2) \bar{R}^2]$.

Now, for the integration with respect to θ , we shall use the approximation (127), $\bar{P}(c) = \sqrt{\frac{2}{\pi l_* \sin \theta}} \cos \frac{\theta}{2} \cos(l_* \theta - \frac{\pi}{4})$. This is a good approximation except very close to the point $\theta = 0$, but the integrand in Eq. (194) vanishes at this point anyway. We combine the strongly oscillating functions in (194) and in \bar{P} ,

$$\begin{aligned} \sin[\omega \bar{R} 2 \sin(\theta/2)] \cos(l_* \theta - \pi/4) = \\ \frac{1}{2} \{ \sin[\omega \bar{R} (2 \sin(\theta/2) + c_0 \theta) - \pi/4] + \sin[\omega \bar{R} (2 \sin(\theta/2) - c_0 \theta) + \pi/4] \}. \end{aligned} \quad (195)$$

where $c_0 = l_*/\omega \bar{R} \sim 1$. As θ varies between 0 and π , the first sine is highly oscillatory for $\omega \bar{R} \gg 1$, and therefore is of higher order in $1/\omega \bar{R}$. Hence, we drop this term. We have to evaluate the imaginary part of the integral

$$I_\theta = \int_0^\pi d\theta e^{i\omega \bar{R} [2 \sin(\theta/2) - c_0 \theta] + i\frac{\pi}{4}} K(\theta), \quad (196)$$

with

$$K = \sin \theta \sin(\theta/2) \cos^5(\theta/2) e^{-I_{\text{tot}}} G \sqrt{\frac{2}{\pi l_* \sin \theta}} \quad (197)$$

For $0 < \theta < \pi$ the exponent has a stationary point at $\theta = \theta_0$ such that

$$\cos(\theta_0/2) = c_0 = l_*/\omega \bar{R}, \quad (198)$$

which exists only if $\omega \bar{R} > l_*$ (otherwise the integral is of higher order in $1/\omega \bar{R}$, so to this order we have a Heaviside function). Thus, we obtain

$$I_\theta = \sqrt{\frac{4\pi}{\omega \bar{R} s_0}} e^{i2\omega \bar{R}(s_0 - c_0 \arccos c_0)} K(\theta_0) \Theta(1 - c_0). \quad (199)$$

where $s_0 = \sqrt{1 - c_0^2}$. Taking the imaginary part and replacing in (194), we obtain

$$\Delta^{(1,1)} = \frac{8a^2 l_*^3}{3R_*^5 \omega^4} \int_{l_*/\omega}^\infty d\bar{R} s_0 e^{-I_{\text{tot}}} G \sin[2\omega \bar{R}(s_0 - c_0 \arccos c_0)], \quad (200)$$

with $G = \exp[-(\omega a/l_*)^2 s_0^2 \bar{R}^2]$ and $I_{\text{tot}} = (2\pi \bar{R}^3 / 3R_*^3) (2 + 3s_0 - s_0^3)$.

Finally, we integrate by parts the last integral and we obtain, to lowest order in $1/\omega \bar{R}$,

$$\Delta^{(1,1)} = \frac{4a^2 l_*^3}{3R_*^5 \omega^5} e^{-I_{\text{tot}}} G \cos[2\omega \bar{R}(s_0 - c_0 \arccos c_0)], \quad (201)$$

where the cosine c_0 is evaluated at the limit of integration $\bar{R} = l_*/\omega$, i.e., we have $c_0 = 1$, $s_0 = 0$, and $\arccos c_0 = 0$. This gives Eq. (143).

References

- [1] M. S. Turner and F. Wilczek, *Relic gravitational waves and extended inflation*, *Phys. Rev. Lett.* **65** (1990) 3080–3083.
- [2] LISA collaboration, P. Amaro-Seoane et al., *Laser Interferometer Space Antenna*, 1702.00786.
- [3] B.-H. Liu, L. D. McLerran and N. Turok, *Bubble nucleation and growth at a baryon number producing electroweak phase transition*, *Phys. Rev. D* **46** (1992) 2668–2688.
- [4] N. Turok, *Electroweak bubbles: Nucleation and growth*, *Phys. Rev. Lett.* **68** (1992) 1803–1806.
- [5] M. Dine, R. G. Leigh, P. Y. Huet, A. D. Linde and D. A. Linde, *Towards the theory of the electroweak phase transition*, *Phys. Rev. D* **46** (1992) 550–571, [hep-ph/9203203].
- [6] S. Y. Khlebnikov, *Fluctuation - dissipation formula for bubble wall velocity*, *Phys. Rev. D* **46** (1992) 3223–3226.
- [7] P. B. Arnold, *One loop fluctuation - dissipation formula for bubble wall velocity*, *Phys. Rev. D* **48** (1993) 1539–1545, [hep-ph/9302258].
- [8] G. D. Moore and T. Prokopec, *Bubble wall velocity in a first order electroweak phase transition*, *Phys. Rev. Lett.* **75** (1995) 777–780, [hep-ph/9503296].
- [9] G. D. Moore and T. Prokopec, *How fast can the wall move? A Study of the electroweak phase transition dynamics*, *Phys. Rev. D* **52** (1995) 7182–7204, [hep-ph/9506475].
- [10] D. Bodeker and G. D. Moore, *Can electroweak bubble walls run away?*, *JCAP* **05** (2009) 009, [0903.4099].
- [11] D. Bodeker and G. D. Moore, *Electroweak Bubble Wall Speed Limit*, *JCAP* **05** (2017) 025, [1703.08215].
- [12] A. Azatov and M. Vanvlasselaer, *Bubble wall velocity: heavy physics effects*, *JCAP* **01** (2021) 058, [2010.02590].
- [13] B. Link, *Deflagration instability in the quark - hadron phase transition*, *Phys. Rev. Lett.* **68** (1992) 2425–2428.
- [14] P. Y. Huet, K. Kajantie, R. G. Leigh, B.-H. Liu and L. D. McLerran, *Hydrodynamic stability analysis of burning bubbles in electroweak theory and in QCD*, *Phys. Rev.* **D48** (1993) 2477–2492, [hep-ph/9212224].

- [15] A. Megevand and F. A. Membiela, *Stability of cosmological deflagration fronts*, *Phys. Rev.* **D89** (2014) 103507, [1311.2453].
- [16] A. Megevand, F. A. Membiela and A. D. Sanchez, *Lower bound on the electroweak wall velocity from hydrodynamic instability*, *JCAP* **03** (2015) 051, [1412.8064].
- [17] A. Kosowsky, M. S. Turner and R. Watkins, *Gravitational waves from first order cosmological phase transitions*, *Phys. Rev. Lett.* **69** (1992) 2026–2029.
- [18] A. Kosowsky, M. S. Turner and R. Watkins, *Gravitational radiation from colliding vacuum bubbles*, *Phys. Rev. D* **45** (1992) 4514–4535.
- [19] M. Kamionkowski, A. Kosowsky and M. S. Turner, *Gravitational radiation from first order phase transitions*, *Phys. Rev. D* **49** (1994) 2837–2851, [astro-ph/9310044].
- [20] A. D. Dolgov, D. Grasso and A. Nicolis, *Relic backgrounds of gravitational waves from cosmic turbulence*, *Phys. Rev. D* **66** (2002) 103505, [astro-ph/0206461].
- [21] A. Kosowsky, A. Mack and T. Kahniashvili, *Gravitational radiation from cosmological turbulence*, *Phys. Rev. D* **66** (2002) 024030, [astro-ph/0111483].
- [22] G. Gogoberidze, T. Kahniashvili and A. Kosowsky, *The Spectrum of Gravitational Radiation from Primordial Turbulence*, *Phys. Rev. D* **76** (2007) 083002, [0705.1733].
- [23] C. Caprini, R. Durrer and G. Servant, *The stochastic gravitational wave background from turbulence and magnetic fields generated by a first-order phase transition*, *JCAP* **12** (2009) 024, [0909.0622].
- [24] T. Kahniashvili, L. Kisslinger and T. Stevens, *Gravitational Radiation Generated by Magnetic Fields in Cosmological Phase Transitions*, *Phys. Rev. D* **81** (2010) 023004, [0905.0643].
- [25] L. Kisslinger and T. Kahniashvili, *Polarized Gravitational Waves from Cosmological Phase Transitions*, *Phys. Rev. D* **92** (2015) 043006, [1505.03680].
- [26] P. Niksa, M. Schlexer and G. Sigl, *Gravitational Waves produced by Compressible MHD Turbulence from Cosmological Phase Transitions*, *Class. Quant. Grav.* **35** (2018) 144001, [1803.02271].
- [27] A. Roper Pol, S. Mandal, A. Brandenburg, T. Kahniashvili and A. Kosowsky, *Numerical simulations of gravitational waves from early-universe turbulence*, *Phys. Rev. D* **102** (2020) 083512, [1903.08585].
- [28] M. Hindmarsh, S. J. Huber, K. Rummukainen and D. J. Weir, *Gravitational waves from the sound of a first order phase transition*, *Phys. Rev. Lett.* **112** (2014) 041301, [1304.2433].

- [29] J. T. Giblin and J. B. Mertens, *Gravitational radiation from first-order phase transitions in the presence of a fluid*, *Phys. Rev. D* **90** (2014) 023532, [1405.4005].
- [30] M. Hindmarsh, S. J. Huber, K. Rummukainen and D. J. Weir, *Numerical simulations of acoustically generated gravitational waves at a first order phase transition*, *Phys. Rev. D* **92** (2015) 123009, [1504.03291].
- [31] M. Hindmarsh, S. J. Huber, K. Rummukainen and D. J. Weir, *Shape of the acoustic gravitational wave power spectrum from a first order phase transition*, *Phys. Rev. D* **96** (2017) 103520, [1704.05871].
- [32] M. Hindmarsh, *Sound shell model for acoustic gravitational wave production at a first-order phase transition in the early Universe*, *Phys. Rev. Lett.* **120** (2018) 071301, [1608.04735].
- [33] M. Hindmarsh and M. Hijazi, *Gravitational waves from first order cosmological phase transitions in the Sound Shell Model*, *JCAP* **12** (2019) 062, [1909.10040].
- [34] H.-K. Guo, K. Sinha, D. Vagie and G. White, *Phase Transitions in an Expanding Universe: Stochastic Gravitational Waves in Standard and Non-Standard Histories*, *JCAP* **01** (2021) 001, [2007.08537].
- [35] A. Kosowsky and M. S. Turner, *Gravitational radiation from colliding vacuum bubbles: envelope approximation to many bubble collisions*, *Phys. Rev.* **D47** (1993) 4372–4391, [astro-ph/9211004].
- [36] S. J. Huber and T. Konstandin, *Gravitational Wave Production by Collisions: More Bubbles*, *JCAP* **0809** (2008) 022, [0806.1828].
- [37] R. Jinno and M. Takimoto, *Gravitational waves from bubble collisions: An analytic derivation*, *Phys. Rev.* **D95** (2017) 024009, [1605.01403].
- [38] C. Caprini, R. Durrer and G. Servant, *Gravitational wave generation from bubble collisions in first-order phase transitions: An analytic approach*, *Phys. Rev.* **D77** (2008) 124015, [0711.2593].
- [39] R. Jinno and M. Takimoto, *Gravitational waves from bubble dynamics: beyond the envelope*, *Journal of Cosmology and Astroparticle Physics* **2019** (jan, 2019) 060–060.
- [40] T. Konstandin, *Gravitational radiation from a bulk flow model*, *JCAP* **03** (2018) 047, [1712.06869].
- [41] A. H. Guth and S. Tye, *Phase Transitions and Magnetic Monopole Production in the Very Early Universe*, *Phys. Rev. Lett.* **44** (1980) 631.
- [42] A. H. Guth and E. J. Weinberg, *Cosmological Consequences of a First Order Phase Transition in the SU(5) Grand Unified Model*, *Phys. Rev.* **D23** (1981) 876.

- [43] M. S. Turner, E. J. Weinberg and L. M. Widrow, *Bubble nucleation in first order inflation and other cosmological phase transitions*, *Phys. Rev.* **D46** (1992) 2384–2403.
- [44] A. Mégevand and F. A. Membiela, *Bubble wall correlations in cosmological phase transitions*, *Phys. Rev. D* **102** (2020) 103514, [2008.01873].
- [45] A. Mégevand, *Friction forces on phase transition fronts*, *JCAP* **07** (2013) 045, [1303.4233].
- [46] L. Leitaó and A. Megevand, *Hydrodynamics of ultra-relativistic bubble walls*, *Nucl. Phys.* **B905** (2016) 45–72, [1510.07747].
- [47] A. Megevand, *Gravitational waves from deflagration bubbles in first-order phase transitions*, *Phys. Rev. D* **78** (2008) 084003, [0804.0391].
- [48] J. R. Espinosa, T. Konstandin, J. M. No and G. Servant, *Energy Budget of Cosmological First-order Phase Transitions*, *JCAP* **06** (2010) 028, [1004.4187].
- [49] L. Leitaó and A. Megevand, *Spherical and non-spherical bubbles in cosmological phase transitions*, *Nucl. Phys. B* **844** (2011) 450–470, [1010.2134].
- [50] L. Leitaó and A. Megevand, *Hydrodynamics of phase transition fronts and the speed of sound in the plasma*, *Nucl. Phys. B* **891** (2015) 159–199, [1410.3875].
- [51] J. Ellis, M. Lewicki, J. M. No and V. Vaskonen, *Gravitational wave energy budget in strongly supercooled phase transitions*, *JCAP* **06** (2019) 024, [1903.09642].
- [52] J. Ellis, M. Lewicki and V. Vaskonen, *Updated predictions for gravitational waves produced in a strongly supercooled phase transition*, *JCAP* **11** (2020) 020, [2007.15586].
- [53] F. Giese, T. Konstandin and J. van de Vis, *Model-independent energy budget of cosmological first-order phase transitions—A sound argument to go beyond the bag model*, *JCAP* **07** (2020) 057, [2004.06995].
- [54] F. Giese, T. Konstandin, K. Schmitz and J. Van De Vis, *Model-independent energy budget for LISA*, *JCAP* **01** (2021) 072, [2010.09744].
- [55] L. Leitaó and A. Megevand, *Gravitational waves from a very strong electroweak phase transition*, *JCAP* **05** (2016) 037, [1512.08962].
- [56] C. Caprini et al., *Science with the space-based interferometer eLISA. II: Gravitational waves from cosmological phase transitions*, *JCAP* **04** (2016) 001, [1512.06239].
- [57] A. Megevand and A. Membiela, *Model-independent features of gravitational waves from bubble collisions*, 2108.07034.

- [58] S. Safran, *Statistical Thermodynamics of Surfaces, Interfaces, and Membranes*. Frontiers in physics. Addison-Wesley Pub., 1994.
- [59] V. Bychkov and M. Liberman, *Dynamics and stability of premixed flames*, *Physics Reports* **325** (2000) 115–237.
- [60] K. Freese and F. C. Adams, *Hadron Bubble Evolution Into the Quark Sea*, *Phys. Rev. D* **41** (1990) 2449.
- [61] D. J. Weir, *Revisiting the envelope approximation: gravitational waves from bubble collisions*, *Phys. Rev. D* **93** (2016) 124037, [1604.08429].
- [62] D. Cutting, M. Hindmarsh and D. J. Weir, *Gravitational waves from vacuum first-order phase transitions: from the envelope to the lattice*, *Phys. Rev. D* **97** (2018) 123513, [1802.05712].
- [63] J. Crowder and N. J. Cornish, *Beyond lisa: Exploring future gravitational wave missions*, *Phys. Rev. D* **72** (Oct, 2005) 083005.
- [64] S. Kawamura, T. Nakamura, M. Ando, N. Seto, K. Tsubono, K. Numata et al., *The japanese space gravitational wave antenna—DECIGO*, *Classical and Quantum Gravity* **23** (mar, 2006) S125–S131.
- [65] M. Punturo, M. Abernathy, F. Acernese, B. Allen, N. Andersson, K. Arun et al., *The einstein telescope: a third-generation gravitational wave observatory*, *Classical and Quantum Gravity* **27** (sep, 2010) 194002.
- [66] AEDGE collaboration, Y. A. El-Neaj et al., *AEDGE: Atomic Experiment for Dark Matter and Gravity Exploration in Space*, *EPJ Quant. Technol.* **7** (2020) 6, [1908.00802].
- [67] S. Weinberg, *Gravitation and Cosmology: Principles and Applications of the General Theory of Relativity*. Wiley, New York, NY, 1972.
- [68] N. Van Kampen, *Stochastic Processes in Physics and Chemistry*. North-Holland Personal Library. Elsevier Science, 3rd ed., 2007.